2020-2021 FSAE Internal Combustion Engine Race Car

A Major Qualifying Project

Submitted to the Faculty of the

WORCESTER POLYTECHNIC INSTITUTE

In partial fulfillment of the requirements for the degree of

Bachelor of Science

By

Evan Karl	Mechanical Engineering, Computer Science
Nicholas Kenny	Mechanical Engineering
Danielle Lavigne	Mechanical Engineering
Benjamin Watkins	Mechanical Engineering

Abstract

The 2020-2021 Internal Combustion Engine FSAE team worked to finish the design, manufacturing and assembly of the 2019 racecar. This project represents a continuation of the 2019-20 car left incomplete due to covid. Our team redesigned the suspension architecture, braking system, drivetrain mounting, exhaust system, and aerodynamic body work. The suspension architecture was revised to allow for more adjustability. The braking system redesign included changes to rotor thicknesses, allowing for better thermal performance and ease of assembly. The drivetrain mounting solutions were redesigned to dampen vibration and allow for alignment of the differential. The exhaust system was improved by removing unnecessary weight and complication. In the future MQP students working on this project can assemble the parts we've redesigned into a fully functioning race car in preparation for the competition next year.

Acknowledgements

Our team's completion of this MQP would not have been possible without the invaluable help of the following people:

- Our advisor **Professor Daniello** for his help, guidance, and perseverance through the multitude of challenges we faced throughout the term. Your feedback during our weekly meetings ensured the team stayed on track to accomplish our goals.
- **Molly Clem** for her assistance in manufacturing parts for the car, and always bringing an enthusiastic attitude to the shop.
- **Kyle Postans and Trevor Shrady** for their helping hands in the engine mounting process.
- **James Loiselle** for his plethora of experience and guidance with Esprit and the machines in Washburn.
- **Ian Anderson** for his help machining and for teaching the team how to TIG weld.
- **Professor Stabile** for his help with ANSYS

Table of Contents

List of Figures

Executive Summary

This project represents a continuation of the 2019-2020 internal combustion racecar left incomplete due to Covid. The goal of this MQP was to complete the car, so it can be used as a learning tool for club members.

We focused our efforts on the suspension, engine mounting, brakes, aerodynamics, and exhaust. For each of these areas, we first had to familiarize ourselves with the existing designs, and modify them as necessary. Then, we completed as much manufacturing and assembly as we could with the time we had.

For the suspension, we first completed a significant redesign. The original design called for machined control arms, but we redesigned the suspension around welded control arms for an increase in adjustability in the system and improved structural integrity. We then manufactured everything in the suspension except for the front uprights, and began assembly.

For the engine and drivetrain mounts, we finished mounting the engine and redesigned the differential mounts for improved strength. We also re-mounted the differential.

For the braking system, we decreased the width of the rear rotors, because the calipers that had been purchased were of a smaller width than the front. We completed machining on the brake rotors.

For the aerodynamic system, we designed and analyzed an aerodynamic package consisting of a nose cone and side pods. We also analyzed potential designs for a rear wing and wind shield, but found them to be unsuitable.

All future work to complete assembly is outlined in the Future Work section. This includes part lists, machining processes, and assembly instructions.

Section 1: Background and Literature Review

1.1 Introduction

Formula SAE (Society of Automotive Engineers), or FSAE for short, is an international competition where teams of undergraduate and graduate students compete to "conceive, design, fabricate, develop, and compete with small, formula-style vehicles" (Formula, 2021). University teams like our own at WPI congregate on an annual basis to compete in different events. There are many components to the FSAE competition, including both static and dynamic events which judge everything from the team's presentation of their design to the handling, acceleration, and fuel efficiency of the car. Static events include a presentation of the car's design, cost of the overall car, and judgement of the car design itself. Sponsoring automotive companies may also have their own components to the overall competition, such as best use of E-85 fuel, recyclability, best use of electronics, etc. Within the dynamic portion of the competition race cars and their drivers push their cars to the limit in acceleration, skid pad, autocross, endurance and efficiency events. Formula SAE events are designed to measure and quantify undergraduate engineering students' ability to collaboratively innovate, all the while creating an environment where they learn important skills along the process and build lasting career networking within the automotive industry.

WPI has competed within FSAE for multiple years, and this year's car is carried over from the 2019-2020 season. Last year's MQP team accomplished much of the design work for many systems on the car, including the spaceframe, steering and braking, ergonomics and driver cockpit, and engine cooling. This year's MQP team expanded upon the development of the car, revising designs to ensure manufacturability and compatibility with existing structures. Our team manufactured and assembled parts for the suspension, drivetrain mounts, and braking

system. In addition, our team redesigned portions of the suspension system, aerodynamics, and exhaust system. The following sections will introduce each subsystem and explore a literary review covering their design and industry research.

1.2 Suspension

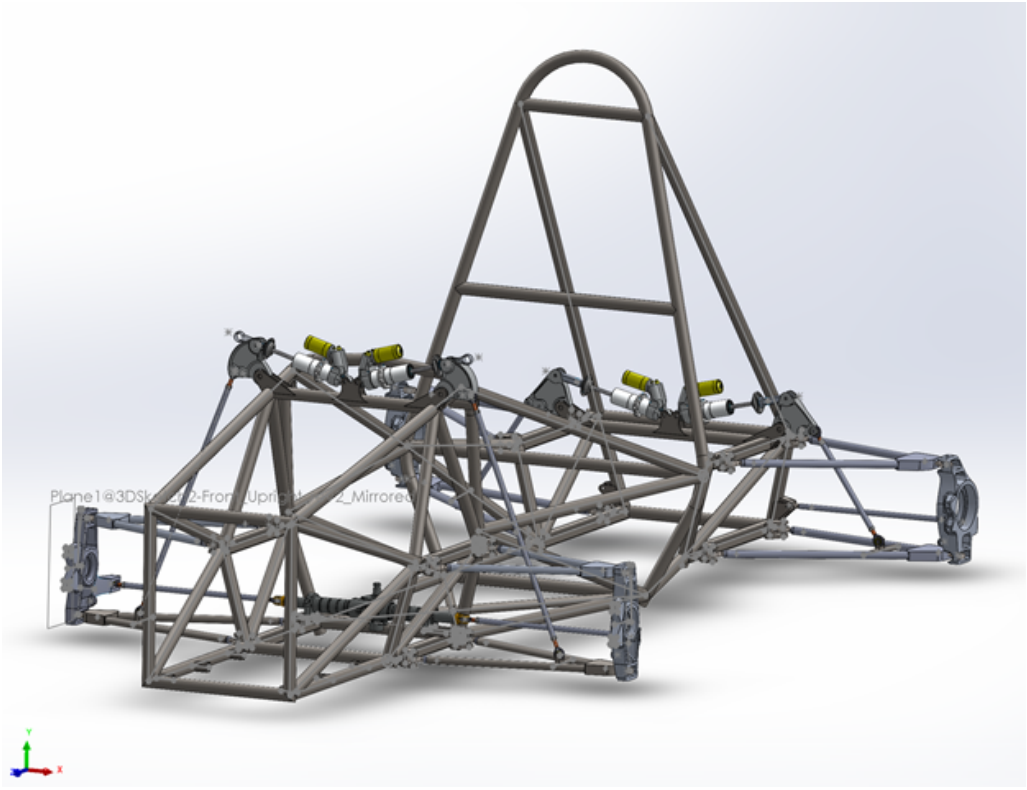

Figure 1: Formula SAE 2021 Internal Combustion Suspension System

1.2.1 System Overview

A vehicle's suspension system is responsible for the translation and control of forces between the tires and the chassis. This control also determines the path of the car through steering inputs and rebound forces (Milliken, 1995).

The suspension system is one of the primary factors in the performance of a vehicle. Various parameters can be set and adjusted, to make up the “setup” or “alignment” of the vehicle. These parameters include but are not limited to, camber angle, castor angle, toe angle, ride height, instant centers, roll centers, and spring rates. Each play a vital role in how a car performs, and their adjustment can help a racecar decrease lap times.

The 2021 Internal combustion suspension system is pictured in Figure 1. Each corner of the car involves two control arms, a pushrod rocker system, a toe link, and an upright.

1.2.2 Control Arms

WPI FSAE has utilized double A-arm suspension geometry, on all recent iterations of racecars. This style of independent suspension involves two control arms to restrict movement, as the knuckle needs to go from 6 degrees of freedom to 1 (Milliken, 1995). To restrict 5 degrees of freedom, we need a system involving 5 tension-compression links. On our double wishbone suspension each control arm accounts for 2 links, and a tierod serves as our fifth link.

In addition to the restriction of motion, control arms are also responsible for camber control and the reaction of brake torque under load. They connect the frame to the wheel assembly and are the connection for the unsprung mass of the racecar (Duff et.al, 2020).

<u>2020 Team Review-</u>

With the 2020 team deciding to transition from the 13” to a 10” wheel, the suspension system had to be redesigned. This change gave the team an opportunity to start over, and address issues with their system they encountered in past iterations. The 2019 car struggled with movement in the linkages, which led to binding in the system under loads. They identified the

cause of this problem was from welding the control arms and cylindrical bearing housings (Duff et.al, 2020).

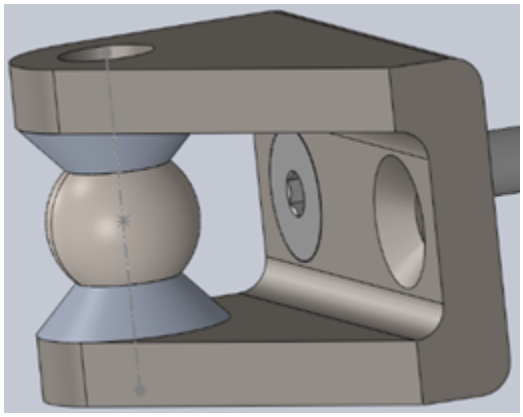

Figure 2: Control arm frame mounting tabs

As a result, the 2020 control arms were slated to be machined via water jet, out of plates of proven aluminum alloy. Machining instead of welding, would help them avoid the welding tolerance issues previously experienced. They attach to the frame via the suspension tabs, using a spherical bearing construction (Figure 2). When progress stopped the control arm designs were finished, and machining was the next step.

Name	Type	Min	Max
Stress1	VON: von Mises Stress	1.636e+04 N/m^2 Node: 47	3.349e+07 N/m^2 Node: 10196

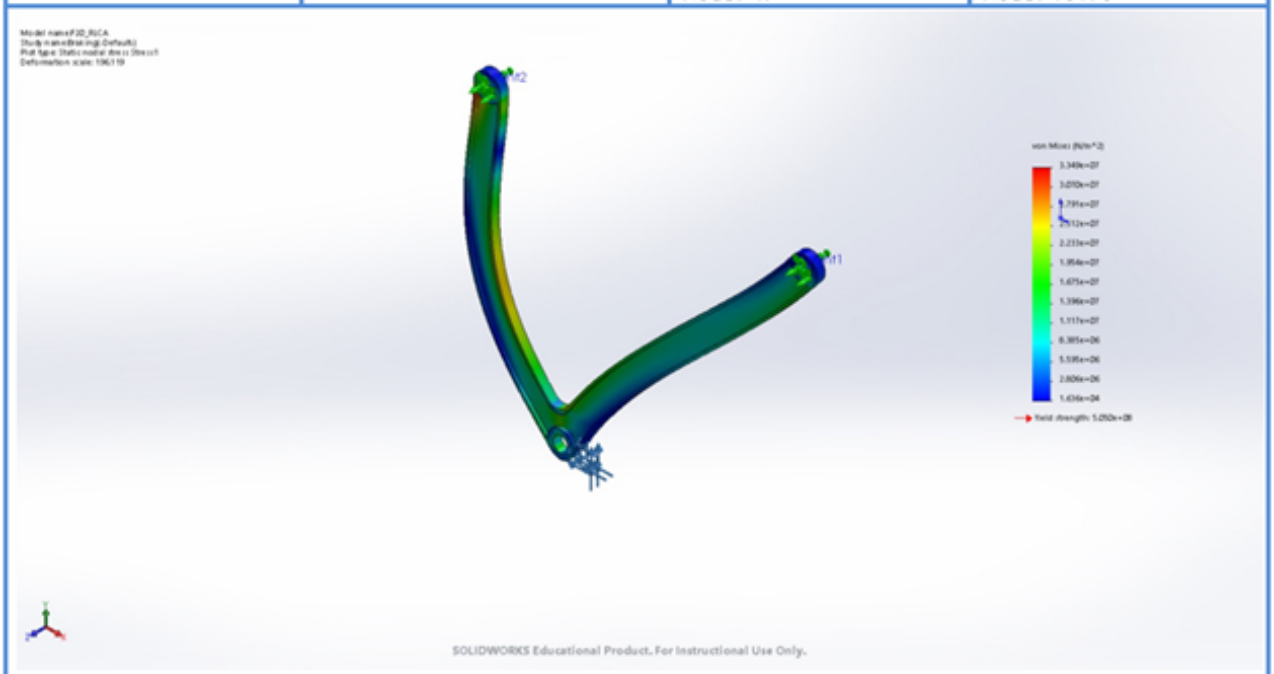

F20_RLCA-Braking-Stress-Stress1

Figure 3: 2020 Control Arm FEA studies (Duff et al.,2020)

1.2.3 Pushrod Rocker System

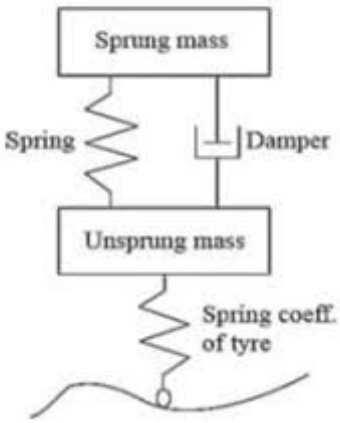

The pushrod rocker system permits the control of the vertical movement of the wheel assembly. This subsystem of the suspension involves the pushrod, rocker, damper, and spring. While springs were used in horse-drawn vehicles, the damper itself was later introduced to the system. Its purpose was to be a link between the unsprung and sprung

Figure 4: Sprung and unsprung masses (Tiwari et. al, 2018)

Masses (Figure 4), controlling oscillation of the sprung mass resulting from various accelerations (Milliken,1995). The rockers themselves redirect the jounce and rebound forces that travel through the pushrod, to the spring. Crucial for a racecar, this type of damping system allows teams to adjust their installation ratio resulting from the spring and damper choice.

2020 Team Review-

Due to the cost of custom order springs, the 2020 team used rocker geometry to provide desired wheel rates. By doing this, they were able to use springs that were already available for purchase or were already owned. With the chosen rocker design, they needed to increase the length of the shock itself. This involved designing custom rod ends for the shock so it could properly attach to the rocker. One rod end was designed for the front assembly, and one was designed for the rear assembly (Duff et.al, 2020).

1.2.4 Uprights

On an FSAE car, the upright is the heart of each wheel assembly. The tierods and control arms connect to the inner portion, while the wheel hub, braking assembly, and tire attach to the outside. As a result, uprights are responsible for addressing various forces generated by the tires and the respective reaction forces. The upright is the means of lateral, longitudinal, and vertical force transfer from the road to the control arms, and onto the pushrod damper system.

2020 Team Review-

The 2020 team completed the upright designs for both the front and rear of the car. They also started to machine out the rear uprights. The main body section of the rears had been bored out, and the holes for the control arm joints, toe rods, and brake calipers needed to be completed.

The front uprights were not started. Per the F20 Final FSAE report, the 2020 team gave us suggestions on how they were planning on machining them.

1.3 Engine and Drivetrain Mounting

The engine and transmission are arguably the most important part of any car. The engine, transmission, and differential that make up the drivetrain create and transfer the force that drives the car forward, translating the linear motion of the pistons within the internal combustion engine into the rotational force that drives the rear wheels. These large, heavy, complex components transfer large forces and subsequent vibrations into the frame of the car through an often overlooked part of the car: the engine and drivetrain mounts. These mounts support the drivetrain, suspending it within the spaceframe behind the driver. They dissipate the vibrations created and ensure the most crucial components of the car do not fall out of it. Differential mounts keep the differential from moving during driveline shocking events, and keep the chain driven motor aligned, ensuring efficient force transmission to the driven wheels.

Engine mounts accomplish two main purposes. The primary job of the engine mounts is to attach the engine, and subsequent driveline components to the car. These mounts must prevent the driveline from breaking free from the subframe through many different scenarios. A common source of shaking is when the car encounters normal bumps in uneven road surfaces. Bumps in the road transfer into the driveline, generating forces that must be managed and dampened. Torque from the engine as it accelerates also contributes to these driveline shocks, creating moments that want to twist the engine out of the engine bay. Driveline and engine mounts must deal with these “low frequency, high amplitude” forces by holding the driveline in place throughout normal operation (Muir, 2019).

No matter how balanced an engine might be internally, every engine generates “high frequency, low amplitude vibrations” through the rotation of it’s camshaft during the thousands of tiny explosions created within the combustion cycles (Muir, 2019). This effect multiplies with the multi-cylinder configurations found in almost every car, with the firing pulses of the different cylinders creating vibrations with respect to each other (Yu et al., 2001). This is the secondary purpose of engine mounts; they dampen vibrations within the driveline, so that they are not transmitted to the car’s occupants. This noise, vibration, and harshness is called NVH, and is an entire field of engineering within car design.

Engine mounts therefore have to balance the stiffness needed to counteract the high amplitude forces of the engine bouncing, and the softness needed to dampen the high frequency vibrations created by nature of the combustion engine. In any car, engine mounts attached to the subframe come in a variety of different materials depending on the application.

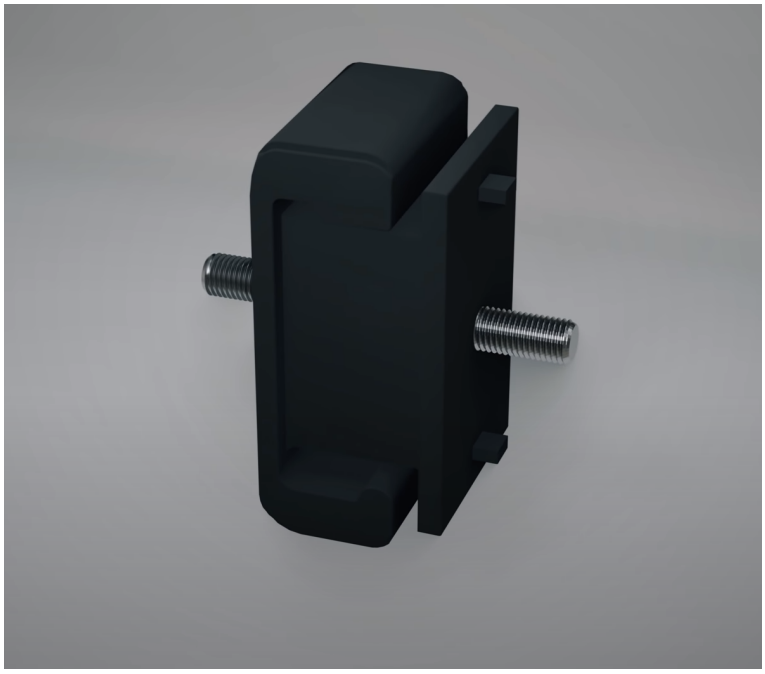

Figure 5: Elastic Rubber Engine Mount (Muir, 2019)

Elastomeric (rubber) mounts are the most commonly used type of mount in the average consumer vehicle, regardless if it is a compact car or pickup truck, these mounts serve a versatile role in holding and isolating the drivetrain. First used in the 1930s (Lord, H.C 1930), they have undergone "significant advancement, such as improved adhesive and extended temperature range" (Yu et al, 2001) in the many decades of their use. They are constructed of two metal plates cast together in a solid block of vibration resistant rubber. Compact, cost effective, and maintenance free, these types of mounts are great at dampening high frequency vibrations at the sacrifice of stiffness for large engine movements and bounces. Despite their shortcomings, elastomeric mounts are popular in many consumer vehicles because the average consumer does not value the stiffness and vibrations found in other mounting systems.

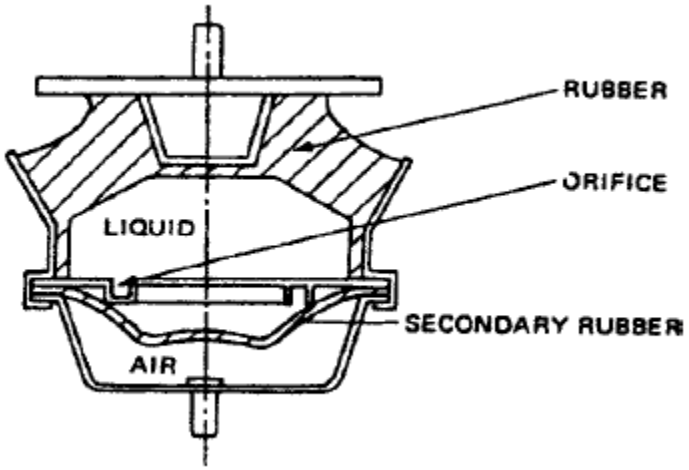

Figure 6: Basic Diagram of a Passive Hydraulic Mount (Yu, 2001)

Another mounting solution developed in hope of creating a good compromise between stiffness and damping is passive hydraulic mounts. These mounts vary in complexity, but the basic premise behind them is to utilize the movement of hydraulic fluid to cause damping at low frequency ranges (Marjoram,1985). This is crucial for the reduction of NVH within front wheel drive, four cylinder ICE cars, as one of the most popular configurations in the world for

consumer vehicles. These engines produce lower frequency vibrations than others, and due to their compact form factor, damping this NVH is important to many car manufacturers. Hydraulic mounts can be tuned by changing their internal construction to dampen certain frequencies more than others (Yu, 2001). They have higher flexibility in the stiffness or frequency response when compared to the equivalent elastomeric mount, making them more capable in a variety of different use cases.

While isolating the driver from NVH is one of the main design objectives for consumer vehicles, race cars have different priorities which do not necessarily align with elastomeric or hydraulic mounting solutions. While these mounts may be effective for noise and vibration dampening, they also allow the engine to flex and twist under its own torque. In a performance oriented situation like racing, that twisting and flexing is lost energy that could be transmitted to the wheels. In racing, stiff mounts like polyurethane and solid mounts are more common. Polyurethane mounts vary in hardness, with some being closer to stiffness as the rubber elastomeric mounts, and harder ones giving very little movement. The most stiff mounting system is solid engine mounting. This is a metal to metal solution, which directly bolts the engine into the subframe. With solid engine mounts, no vibration is dampened and no energy is diffused into the twisting or rocking of the engine.

Engine mounting may be conceptually straight-forward, but as with every system within a car, nothing within its design is simple. There are forces and moments created by uneven road surfaces to consider, vibrations and harshness to dampen, and even the own forces created by the engine the mounts are meant to hold. There is no clear answer, as the final design is entirely dependent on the needs of the end consumer. In a racing situation a stiff mounting system like

polyurethane and solid mounts are most appropriate, and are the best ones to consider for our race car.

1.4 Braking

The purpose of the braking system is to provide a driver with a method to decelerate and stop the vehicle. For the purposes of our Formula SAE racecar, the car is required to lock all four wheels upon depressing the brake pedal. The braking system is also required to provide the driver with the ability to modulate the speed in addition to locking the wheels. To accomplish this, there needs to be two distinct braking circuits in the car: front and rear (Formula, 2021).

2020 Team Review

Before purchasing or designing any components, the 2020 team performed extensive brake calculations in an excel spreadsheet. To determine the force needed to lock the wheels, the team setup a scale, and measured the pressure various club members could exert on the "pedal." This helped them understand the average potential of drivers, and they could make the brakes lock near that pressure. All calculations were done twice, as the front and rear braking circuits needed to be designed (Duff et. al, 2020).

With calculations complete, the team could then design and buy the correct parts for the system. With an increase in wheel size to 10in. The team chose new calipers based on calculated rotor torque. The calipers chosen were ISR 22-048 for the front and ISR 22-049 for the rear. New master cylinders were also chosen that allowed for swiveling in our mounting brackets. The 2019 car had master cylinders that were permanently mounted to a plate.

The new master cylinders were needed as the 2020 and now 2021 car features a new pedal box (Figure 7). Using a balance bar attached to the back of the pedal, two master cylinders are compressed and move respectively as the braking system is used. The 2020 team performed the necessary FEA to ensure the assembly could withstand a 2000 N load at the pedal face, per the FSAE rules (Figure 8).

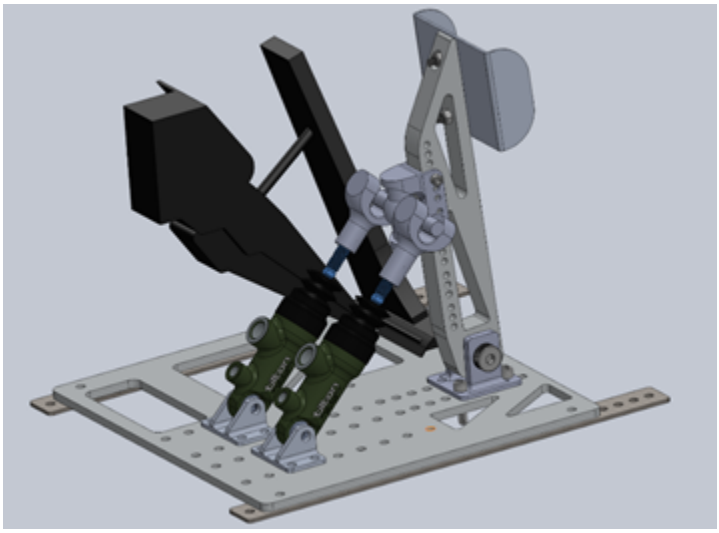

Figure 7: 2021 Pedal box

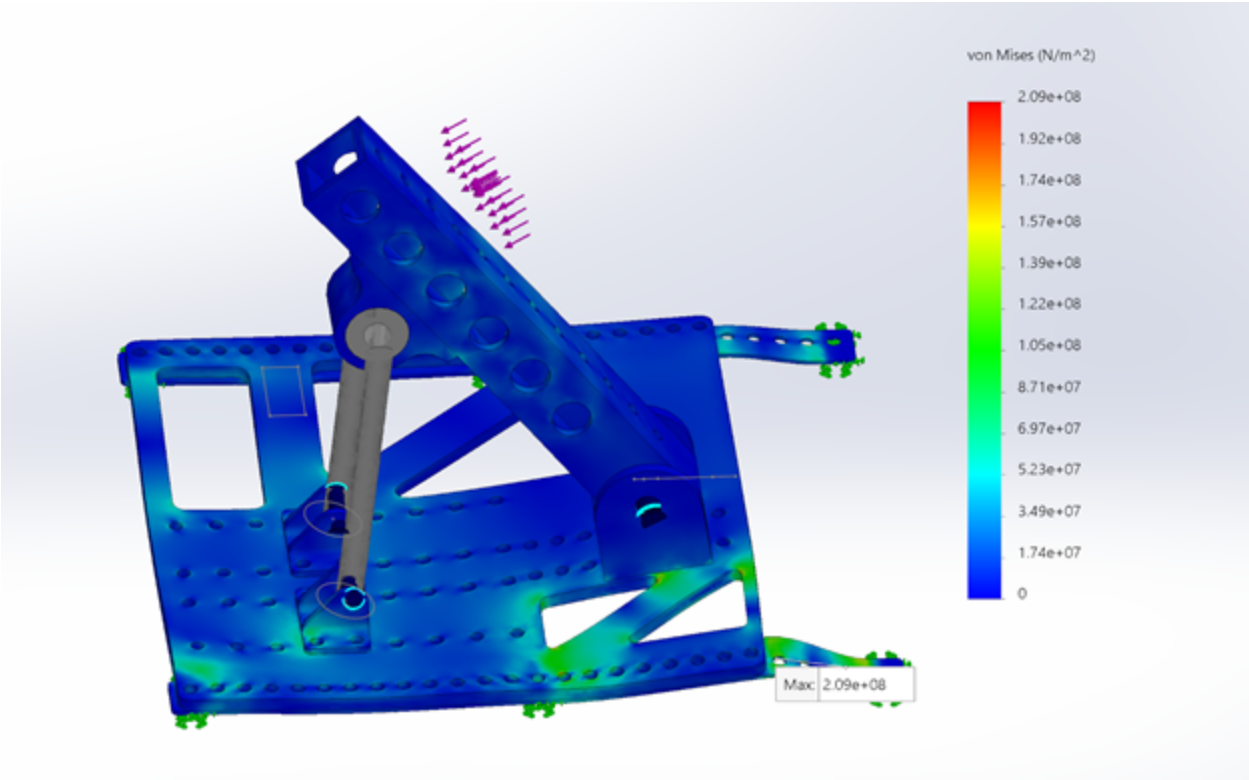

Figure 8: FEA Study on Pedal Box (Duff et. al,2020)

The change to the 10" wheels meant that new brake rotors would be needed. Due to this strange wheel size (but commonly used on FSAE cars), there are few rotors available commercially that could fit inside the wheels (Duff et al, 2020). Those available required changes to other components on the car to become compatible. As a result, the 2020 team decided to design and machine their own brake rotors.

After considering material properties, the team decided to purchase cast iron as it had comparable temperature changes under braking to carbon steel. Cast iron could also be purchased from a local supplier. With the material selected, they then started designing. Once surface area for the brake pads was determined and hub mounting geometry was implemented, they started analyzing performance. The team compared a slotted and drilled rotor. These holes

through the rotor allow for gases to escape, greater surface area for pads to utilize, and weight reduction. Solidworks thermal studies were done to determine the best rotor (Figures 9 and 10).

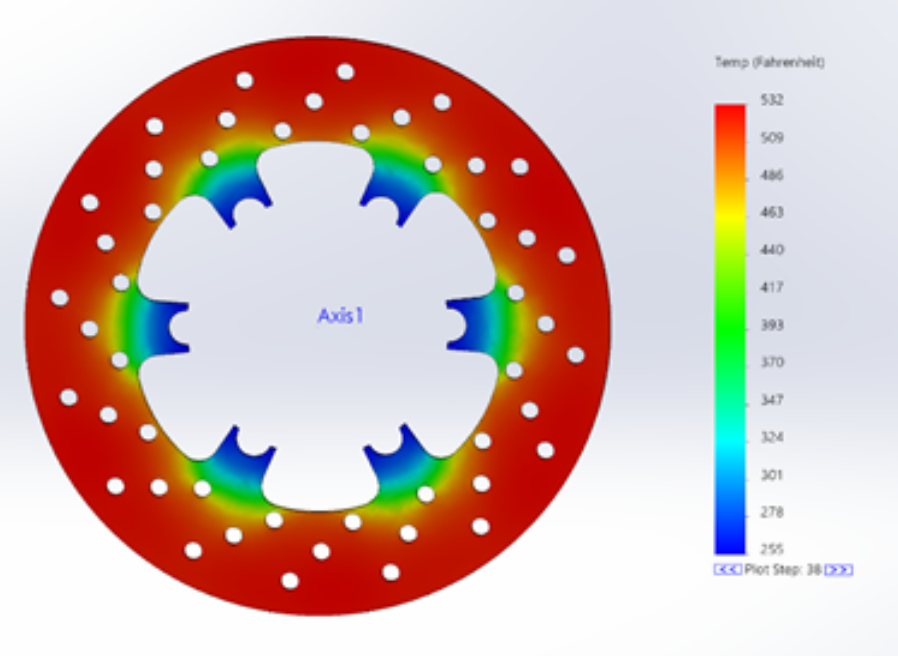

Figure 9: Thermal Study of drilled brake rotor (Duff et al, 2020)

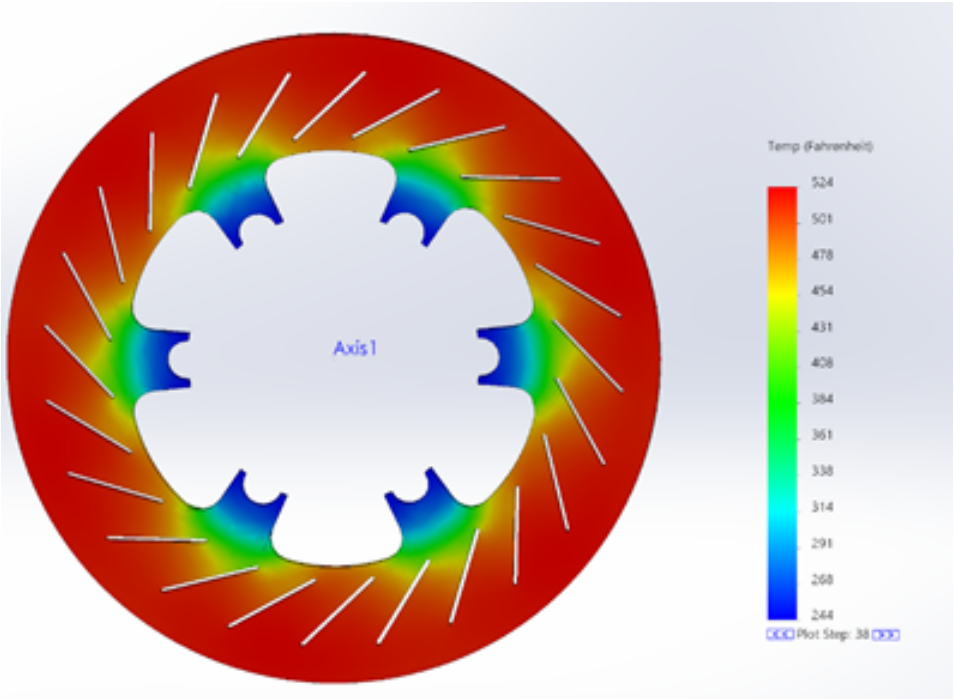

Figure 10: Thermal Study of slotted brake rotor (Duff et. al, 2020)

It was determined that the performance differences were minimal. Due to ease of machining, the drilled rotor was the selected option.

1.5 Aerodynamics

Aerodynamic design of automobiles dates back about 100 years. In the 1920's, car designers began considering the effect that the shape of a car had on its speed; they found that streamlined, teardrop-shaped cars faced less air resistance and thus could go faster. In particular, the 1921 Rumpler "Tropfenwagen" or drop car was able to reach a top speed of 70 mph despite only having a 36 hp engine. (Ketsatis, 2021)

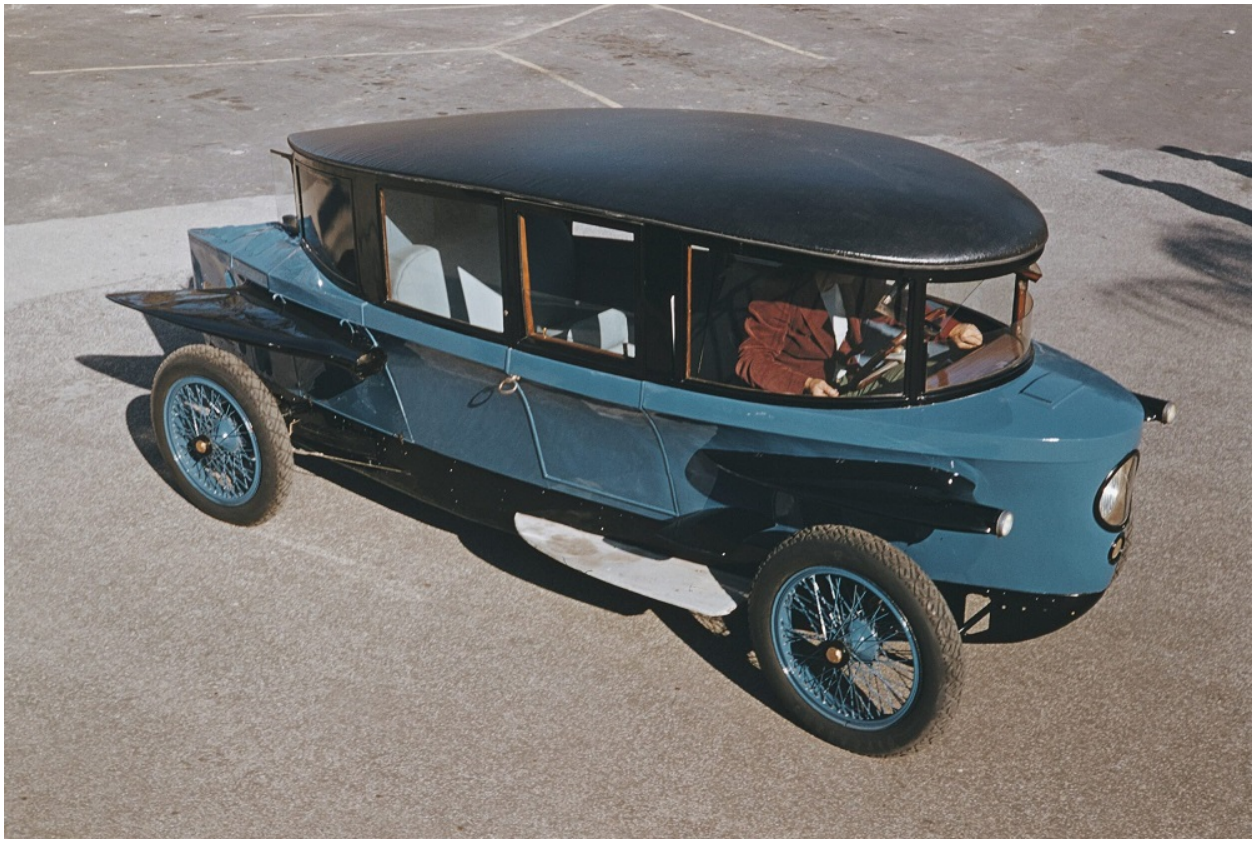

Figure 11: The Tropfenwagen, showing its distinctive tear-drop shape (Ketsatis, 2021)

The influence of this early understanding of aerodynamics could be seen in Auto-Union's grand prix cars of the late 1930's. The success of these car's aerodynamic design allowed them to dominate the sport until the interruption of World War 2. (Vijayenthiran, 2012)

Figure 12: 1939 Auto-Union type D (Vijayenthiran, 2012)

After the war, aerodynamic development continued to streamline cars, reducing their drag. The next major breakthrough was not in efficiency, but downforce; by adding a rear wing, air could be forced upward driving the rear wheels of a car into the pavement and increasing their grip at high speeds. The 1966 Chaparral 2E was a race car that utilized such a wing. Although such high pylon-mounted wings would be banned in most race series in the following years as safety hazards, it demonstrated the power of rear downforce, leading to the ubiquity of rear wings in motorsport today. (Gillies, 2020)

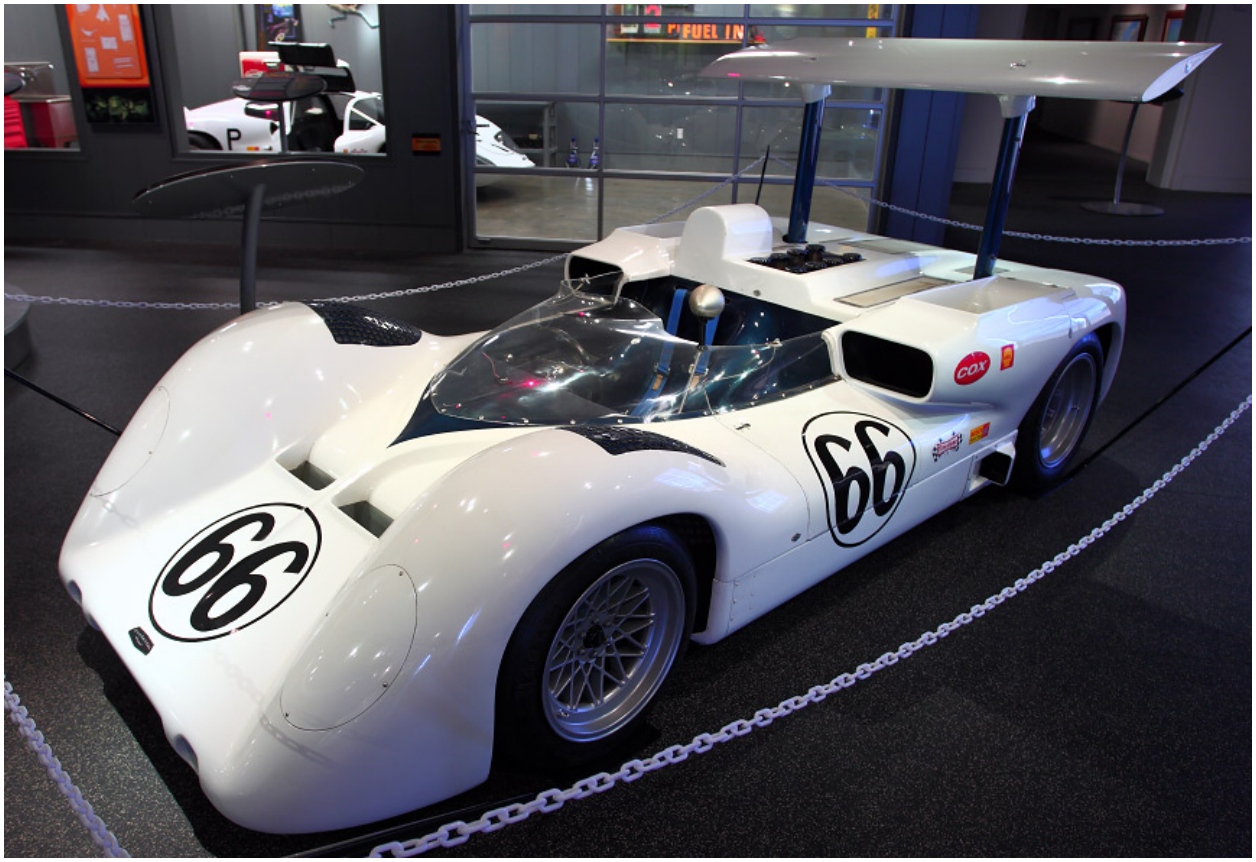

Figure 13: The 1966 Chaparral 2E, showing its rear wing

1.6 Exhaust System

The 2020 FSAE Team designed an exhaust system based off a previous years' design using calculations from "A. Graham Bell's Performance Tuning in Theory and Practice, Four-Strokes", and can be seen below:

P=(850(ED) / RPM) - 3
P=(850(254) / 6000) - 3
P=33 in.

P = Pipe Length (in.)
ED = Angle range in which exhaust valve is open.

ID = (√(cc / (P+3)25))*2.1
ID = (√(449.3 / (32.98+3)25))*2.1
ID =1.5 in.

ID = Inner Exhaust Pipe Diameter
cc = Cylinder Volume (cm^3)

The numbers in these calculations were based off of the specifications of a 2018 Yamaha WR450F engine. They completed their calculations and designs, so all that was left was to manufacture the exhaust system.

1.7 Lap Simulation

With the integration of technology into the automotive performance industry, simulation has become a popular tool. Whether on a professional or student run team, simulation can provide a competitive edge while helping to make more informed engineering decisions. While simulations can be run to see how various systems of a car operate over time, simulation is often used to calculate and compare lap times.

Lap time simulation focuses on the changes in lap time as various parameters of the car are altered. In doing so, the user can use simulation as a method to validate and make design decisions using previous runs as a control/baseline. Professional teams, like those that compete in NASCAR use simulation daily to make minor changes to their setup (camber, castor, toe, spring rates, ride heights, ect.). However for FSAE teams, lap time simulation helps us make major design decisions in the building of the car.

While a lot of the design decisions were already made for the 2021 Internal combustion, a lap simulation tool was developed to help improve the car and to help build future cars. For example in an electric implementation, the club could decide on which motor configuration is best for packaging, performance, and budget using lap simulation to understand the trade off in performance. Furthermore, simulation could be used to track power draw from the accumulator and make size decisions based off the runs.

Section 2: Design Decisions

2.1 Suspension

2.1.1 Control Arms

The internal combustion (IC) car will no longer be competing at the national FSAE competitions. The focus of the club has shifted to the electric implementation, and the IC car will be used as a learning tool for the club members. For reference we still built to the FSAE rulebook, but this shift in purpose affected how the suspension system was finished.

In evaluating the 2020 control arms, it was determined that the geometry of the rear designs would provide a rear track that was shorter than the minimum per the rule book. The decision was made to again redesign the suspension system, this time with adjustability for members of the club to learn about creating a setup for a racecar. Previously all setup parameters were confined to the static construction of the uprights. In addition to the static design, the 2021 suspension has adjustable camber, castor, and toe.

To accomplish this, the control arms reverted to a tube style design with three threaded end links (Figure 14). Instead of welding the arms of the control arms to spherical bearings, they are inserted and welded into a gusset (Figure 15). This helps alleviate the tolerance issues previous FSAE teams experience. The lower control arm features a crossmember for the mounting of the pushrod to the rocker-damper system.

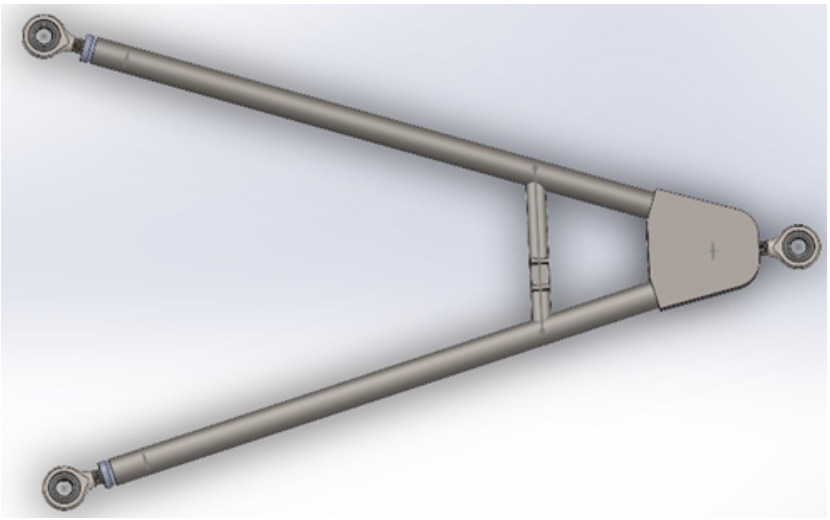

Figure 14: 2021 right front tube lower control arm assembly

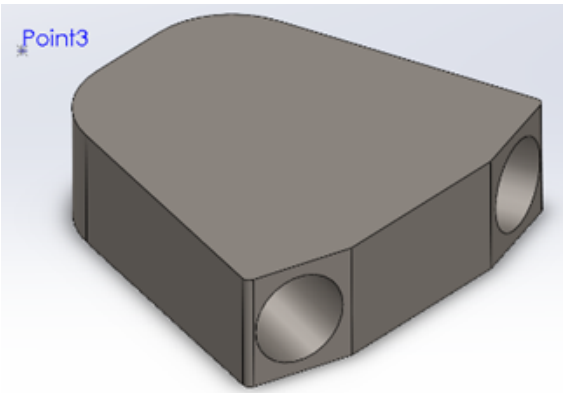

Figure 15: Control arm gusset

A control arm insert is also welded into the end of the arms that attach to the frame, so the end links can be threaded in (Figure 16). This insert is 1.25in long, with a .25in head that extrudes from the control rod end. This extrusion is chamfered, so it can be better welded to the end of the hollow rod once inserted.

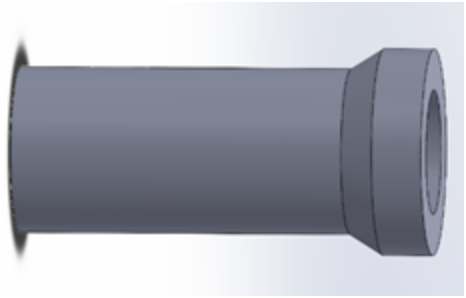

Figure 16: Control arm end insert

Each end link has 0.2” of thread from the end of the control arm or gusset, which starts the car with 0 degrees of camber (Figure 17). It was determined this distance was appropriate as the rest of the 1.25” thread is in the control arm rod for support.

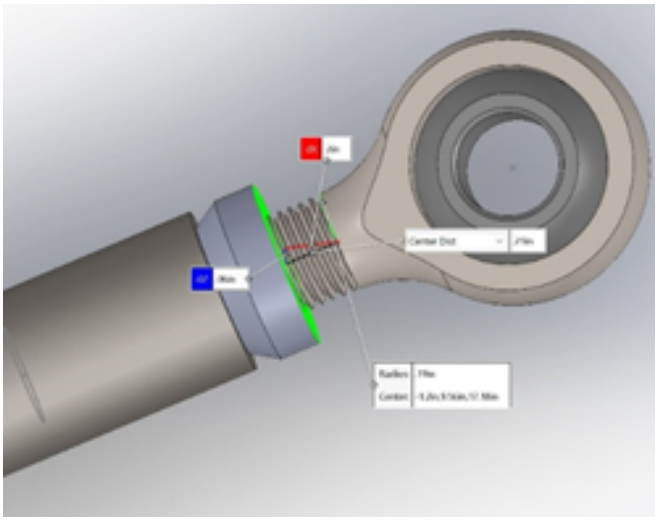

Figure 17: Mounted rod insert with end link 0.2” distance

Furthermore, per drawings in Solidworks (Figure 18), it was found that by bringing the end link of the lower control arm to 0.34” of exposed thread, the car would have -2 degrees of camber. This is a common value for FSAE cars, and by starting the system at 0.2” of thread, there is still enough thread left in the control arm tube to provide adequate support.

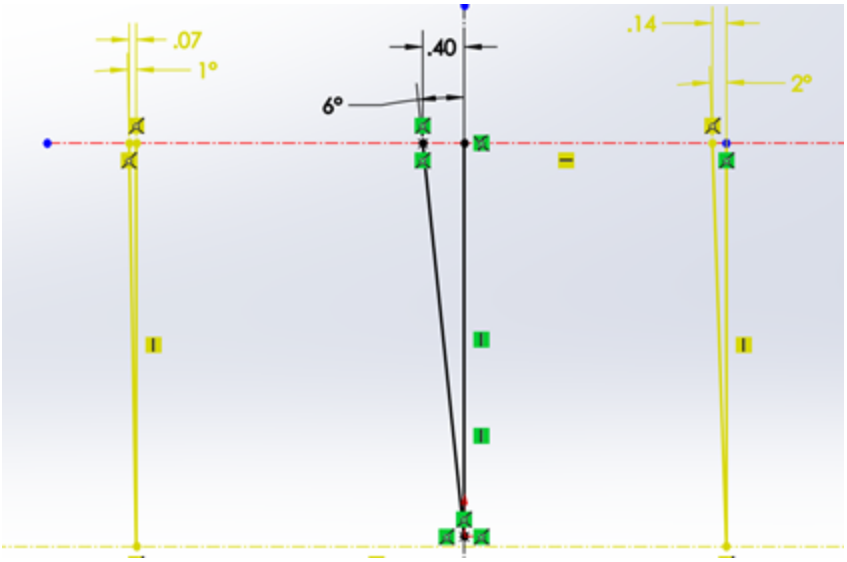

Figure 18: Solidworks camber drawings

The 2021 control arms, and the rest of the suspension system, is made from 4140 steel. The team aimed to use 7075 aluminum alloy tubes, like the sheets the 2020 team had purchased. Because the 2021 team operated on no budget, we were forced to use metal found around the FSAE shop. Thankfully, we were able to find enough 4140 steel tubing to create our control arms. Using Solidworks, FEA was done using 4140 steel to ensure it would have the same results as the intended 7075 aluminum alloy which was previously analyzed in 2020 and again in 2021.

Due to the budget and covid complications through the academic year, the suspension system could not be fully assembled by the submission deadline for the present report. Currently the entire design is finished, all tubes for the control arms have been cut, the gussets and the tube inserts have been machined.

2.1.2 Pushrod Rocker System

The 2021 team used the same pushrod rocker system that the 2020 team intended to use. When progress stopped in 2020, the designs of the pushrods and rockers were supposed to be complete. Enough end links were previously purchased to supply the implementation on all four corners of the car.

Upon initial review, it was clear that the front rocker designs were not complete. By design each rocker had a significant amount of material removed from the side faces for weight reduction. However, one side of the front rockers did not feature this finished weight reduction design. This was completed. Through Solidworks FEA, the 2020 team found that taking material out of the side faces of the part did not negatively affect its strength.

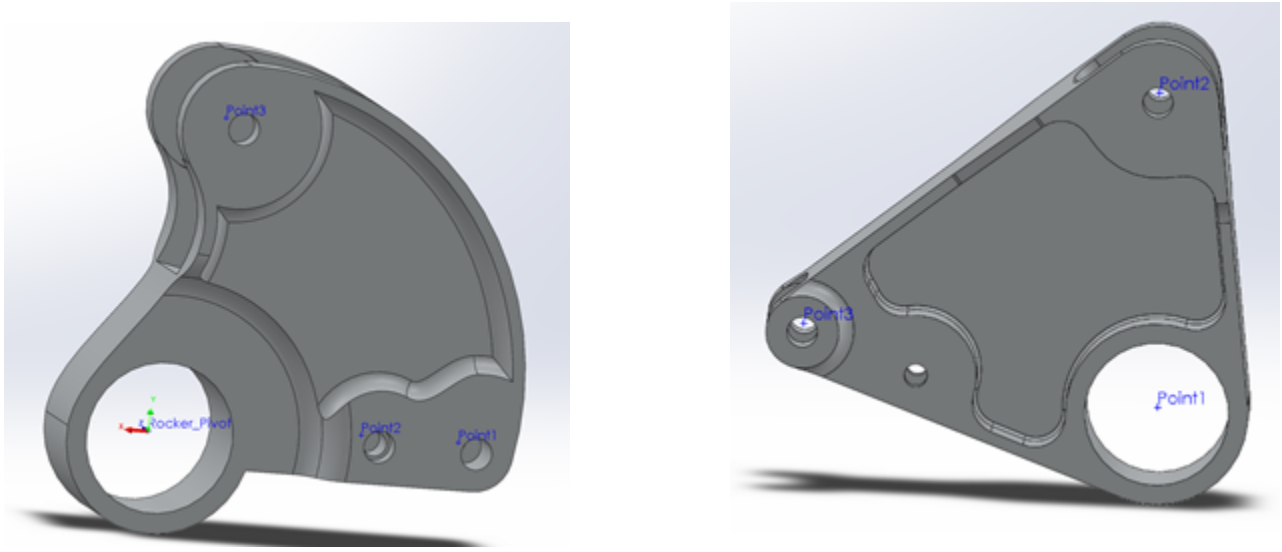

Figure 19: Front and rear rocker designs

Due to the global pandemic we were not able to outsource the machining of the front uprights, which connect the wheel hub to the control arms. The 2020 team intended for the pushrod to be mounted on these uprights, which would cause radial instead of axial loading

(Duff et al., 2020). Through conversation with the alumni design engineer, the team learned the decision to mount on the upright was a poor design choice. In addition, the 2021 team found that having this pushrod mount on the uprights made them impossible to machine with the resources we have at WPI. The decision was then made to add a crossmember to the lower control arm, for the pushrods to be mounted to (Figure 20). This construction is common in the racing industry.

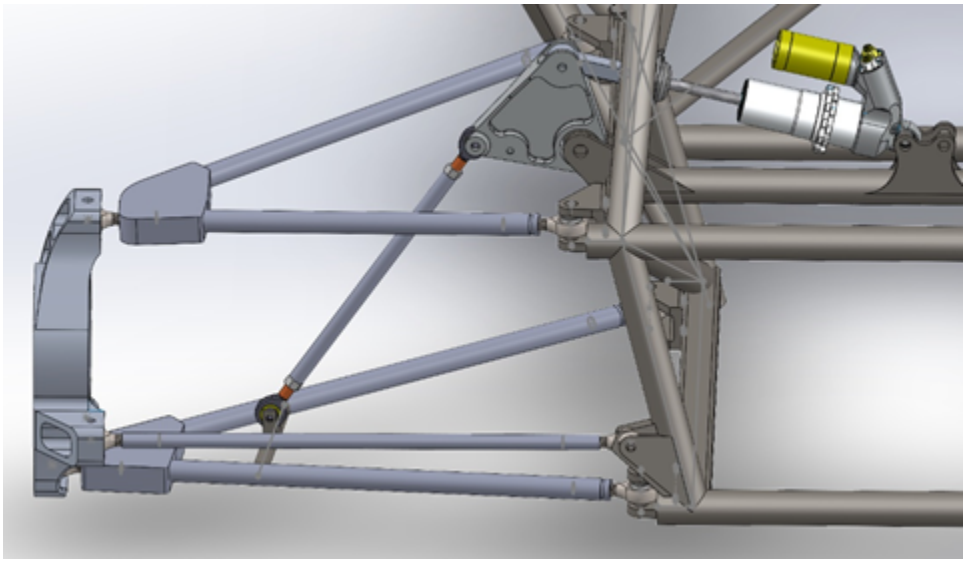

Figure 20: Rear pushrod rocker assembly with lower control arm pushrod mounting

The relocation of the pushrod mounting locations meant the pushrod lengths had to be adjusted. The 2021 team remade the pushrods in Solidworks to adhere to this length change as well as the addition of appropriate end links. By building the front suspension assembly in Solidworks, we were able to adjust the pushrod lengths so the angles between the pushrod and rocker, and rocker and damper were appropriate (Figure 21). The angle between the pushrod and damper should be between 80° and 120° for best load transfer (Vadhe, 2018). However, with the custom rod ends from the 2020 team, the pushrod mounting location on the rocker was

perpendicular to the ground. This meant with the pushrod mounted, motion would not be allowed with the system in a “Z” configuration.

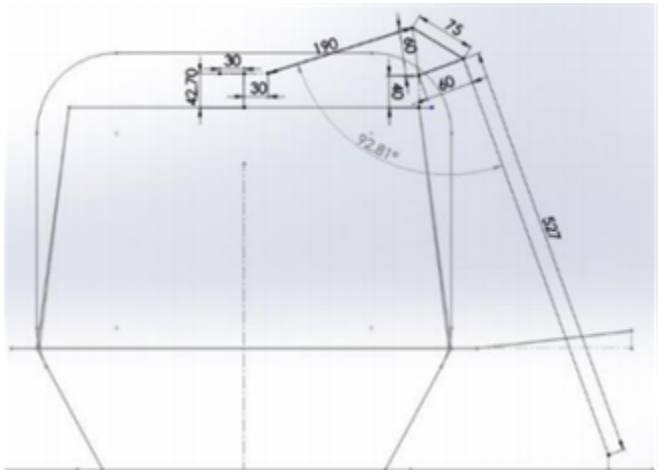

Figure 21: Angle of consideration in the pushrod rocker system (Vadhe, 2018)

This complication occurs regardless of the pushrod mounting location change. It was determined to be an oversight in the front end by the 2020 team, as the rear rod lengths provided the appropriate angles for the rear rockers. The rocker geometry had to be altered so the stock rock ends on the dampers could be used, and the appropriate angle between the damper and pushrod could be achieved. The side face rocker designs also had to be changed once again. The machining methods available through WPI would not allow for certain 90° cuts that were in the designs.

The 2020 team made the decision to use 7075 aluminum alloy for the rockers as they are only being machined and not welded. The pushrods need to have a nut welded on each end for the end links to thread into. The rod body themselves are made out of 4140 steel for this reason.

Understanding that the 7075 aluminum alloy provides significant weight savings (Figure 22), FEA was done to ensure that it was as viable as 4140 steel (Figure 23). Results showed that each material had nearly identical stress and displacement results under an estimated average load. This load was based on the estimated weight off the racecar. Thankfully 7075 aluminum alloy was already purchased, and we could proceed with the rocker machining and cutting of left over pushrod rod stock found in the FSAE shop.

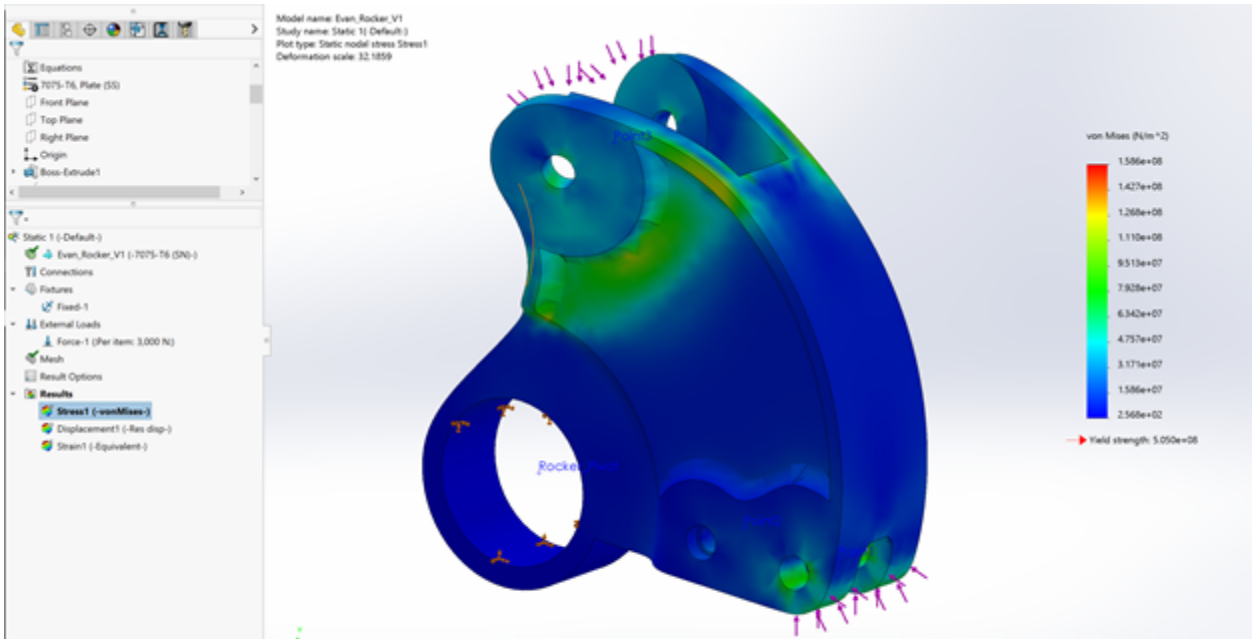

Figure 22: Front rocker FEA study with 7075 Aluminum Alloy

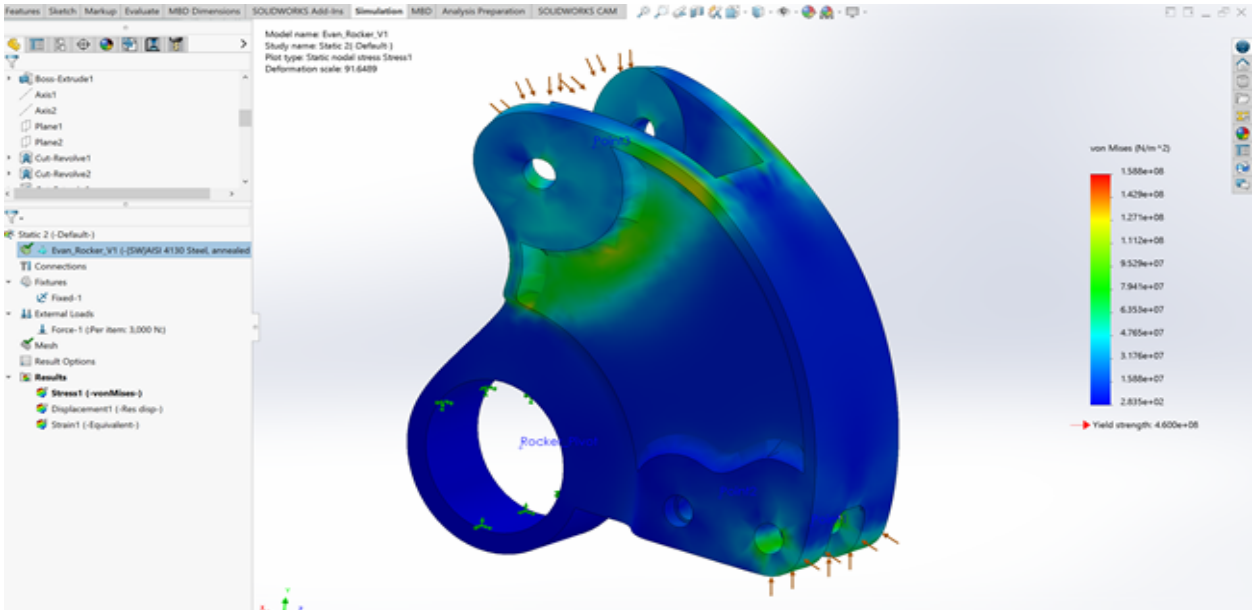

Figure 23: Front rocker FEA study with 4130 Steel

2.1.3 Uprights

The rear uprights had their machining process finished, with minimal complications (Figure 24). Due to the pandemic, the team struggled to have consistent access to the lab and various machine shops. This availability issue and the complexity of the front upright machining process delayed their completion. Currently, the multi-step machining process on the front uprights has begun.

Figure 24: Finished rear uprights

All additional connections on the uprights are via mounting hardware. No welding is needed for this part of the suspension system. As a result, the 2021 team continued with the plans for using the 7075-aluminum alloy stock which was purchased the previous year.

2.2 Engine and Drivetrain Mounting

Two front and two rear engine mounts hold the Yamaha engine and transmission in place within the frame. These are solid mounts, with a focus on creating a stiff connection between the frame and drivetrain with little damping for vibrations and maximum power transfer to the driven wheels. The bulk of the design for the engine and transmission mounting was accomplished by the 2019-2020 FSAE MQP team. The mounts are designed to sustain the peak force of 50lbft of torque from the engine, multiplied through first gear's gear ratio of 2.42,

totaling a maximum of 121lbft of torque. The engine mounts are waterjet from ⅜” thick 7075-T6 plate.

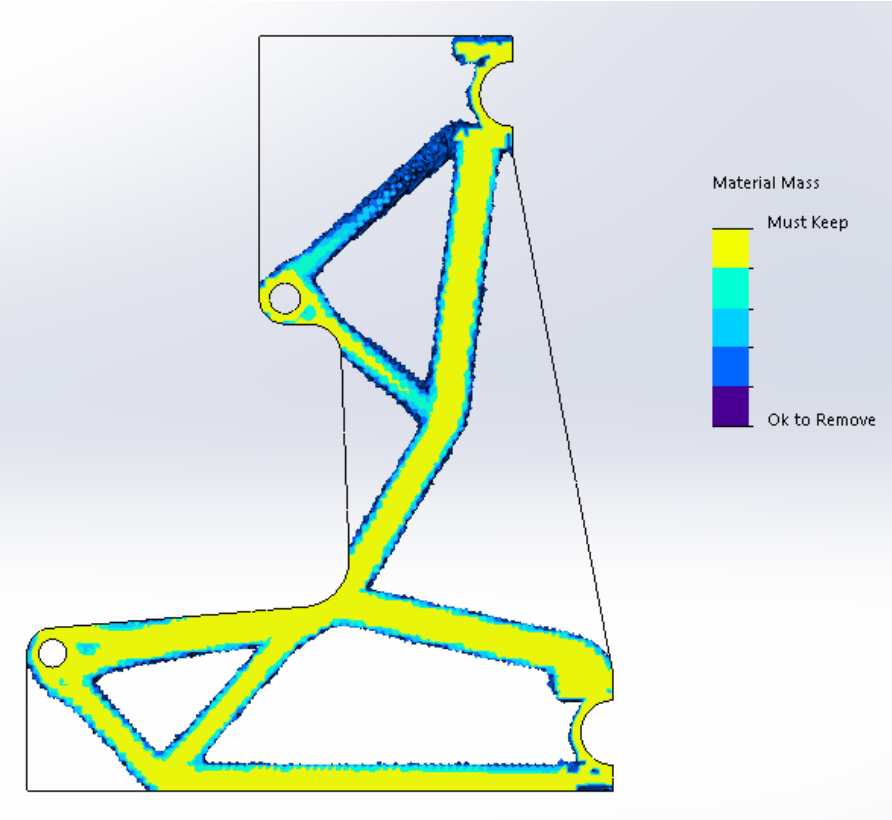

Figure 25: Previous year's front engine mount topology study (FSAE 2019-2020)

The team conducted multiple analysis through solidworks, including a topology study to eliminate excess weight, and a force analysis to make sure the mounts would not buckle under load. The mounts attach to the frame using caps and bolts that hold the cap on and the engine mount in position. To attach to the engine and transmission, a ⅜” threaded rod is slid through holes on the engine and transmission and his held in by lock nuts on either end.

This year, the team's design improved on the previous years' by adding spacers to the engine mounts so that the mounts did not allow the engine to move side to side during operation of the car. To further improve the engine mounts, rubber bushings were added along the

threaded rod. These bushings would dampen any shocks from any uneven track surface, and even provide a minute amount of vibration absorption.

Figure 26: Hillman Rubber Bushings (Hillman Group)

These design decisions were made to maximize the performance of the car while isolating some of the harsher vibrations from the driver, all in hopes of promoting a better score during the dynamic portion of the competition.

While the engine mounts received a design upgrade, the differential mounts and mounting system was completely revamped. Previously the differential was supposed to mount to small steel tabs, which were difficult to weld, difficult to position well, and in the end were structurally weak compared to other solutions. To improve on this design, our team adopted a new mounting bracket to the frame, utilizing parts of the already successful engine mount designs, along with many other improvements shown below:

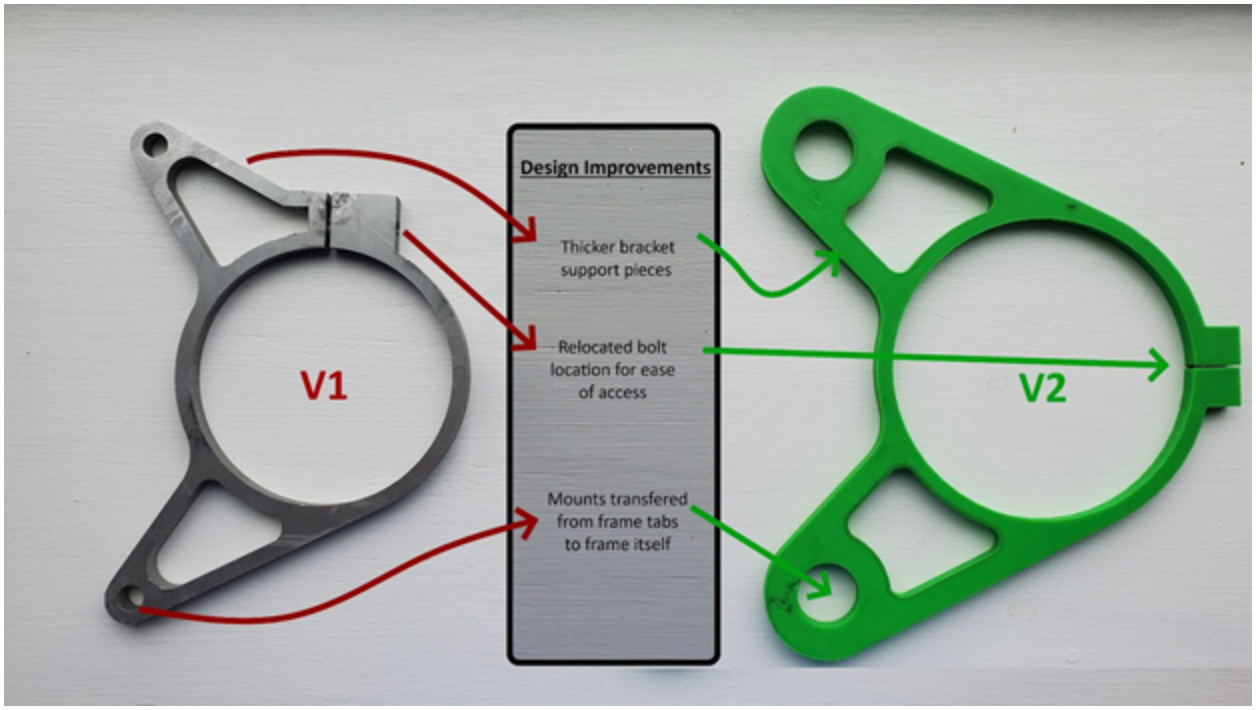

Figure 27: V1 Differential Mount (2019), Improved V2 Differential Mount (2020)

The new design of differential mount attaches to the frame in the same way as the engine mounts, they use a cap and bolt design. Each cap is secured with two 8mm bolts and a set screw through the center of the cap to prevent movement once the final alignment with the drive chain has been set. This design allows for a much quicker alignment process, as both the engine and differential can be positioned freely before being torqued down for racing. The bolt which tightens the collar around the differential body has also been relocated, in order to provide better access for the installer. The bracket supports themselves are thicker, preventing any twist in the mounts during operation. The mounts themselves are structurally more stable, with a 66% increase in thickness of the supporting arms of the mount, from 6mm thick to 10mm. This increase in thickness was necessary to prevent flex or failure during a drivetrain shock event.

2.3 Braking

The braking system was thoroughly designed and ready to be machined when progress stopped for the pandemic. As a result, there was minimal work that needed to be done by our team in terms of design. However, we did find an oversight when starting the machining process on the rotors.

Per design by the manufacturer, the calipers selected required a larger rotor width in the front and a smaller in the rear. This should have been expected, as front calipers are often larger to account for weight transfer under braking. The designs from the 2020 team built to the front caliper width, meaning it would not fit inside the rear calipers. When manufacturing was beginning, the widths were adjusted appropriately. The front rotor width stayed at 0.29in, while the back was reduced to 0.19in.

2.4 Aerodynamics

For the aerodynamic design, we first wanted to reduce drag. To do this, we would need a nose cone to give the car an aerodynamic teardrop shape. Ideally, the nosecone should cleanly split the airflow up and around the chassis.

To analyze the aerodynamic surfaces, we used solidworks flow simulation. We used a design speed of 50 mph. While the car is certainly capable of a higher top speed, due to the tight corners and short straits of the FSAE competition track we felt that 50 mph was a representative track speed.

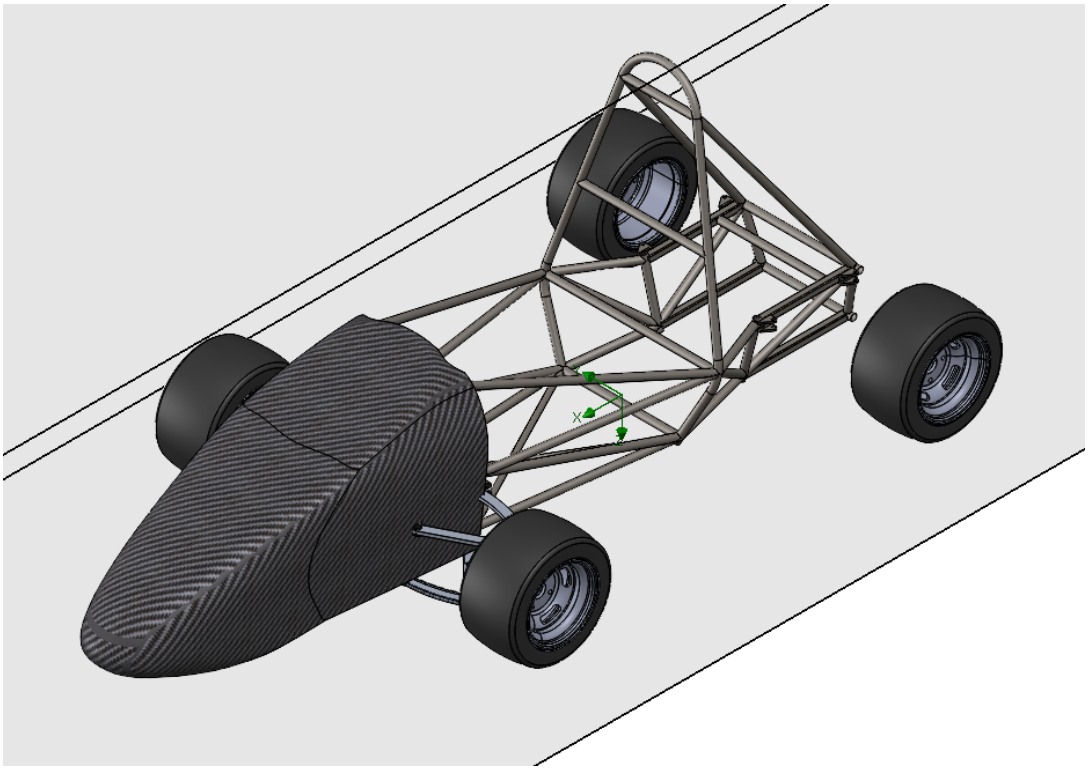

Figure 28: The nose cone

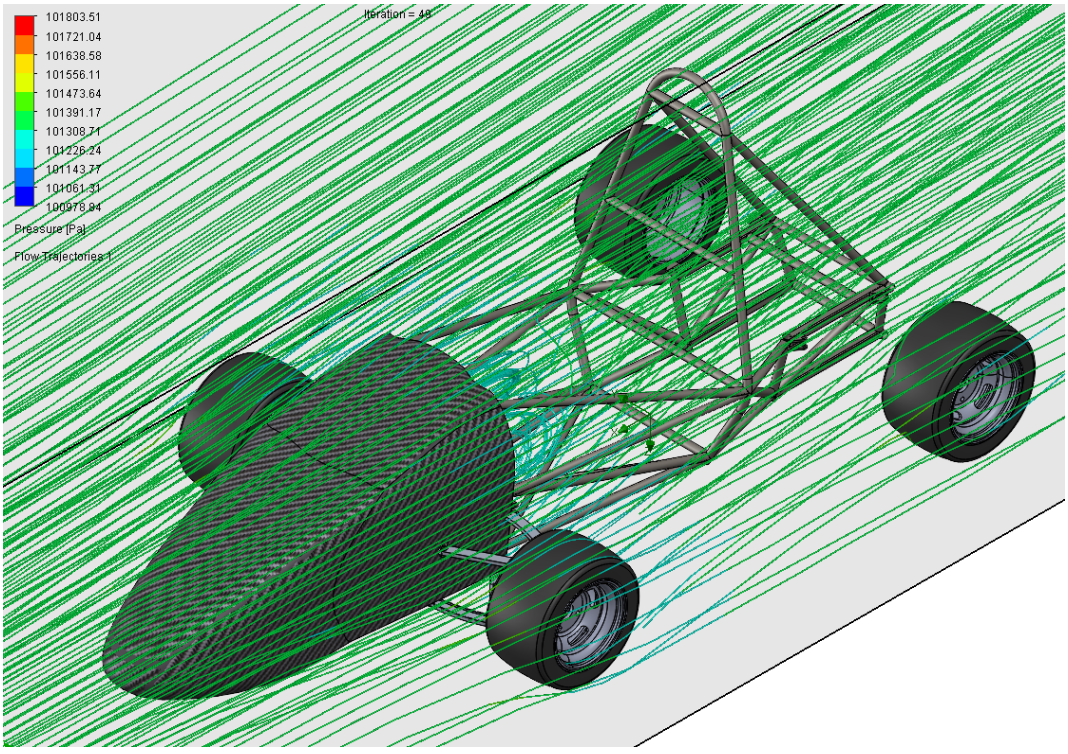

Figure 29: The nose cone flow simulation

This nose cone does a good job of splitting the airflow over and around the front of the car, but it creates turbulent vortices in the driver's enclosure. This will cause driver discomfort as well as creating drag. To solve this issue, we need to add side panels to create a more enclosed driver cabin.

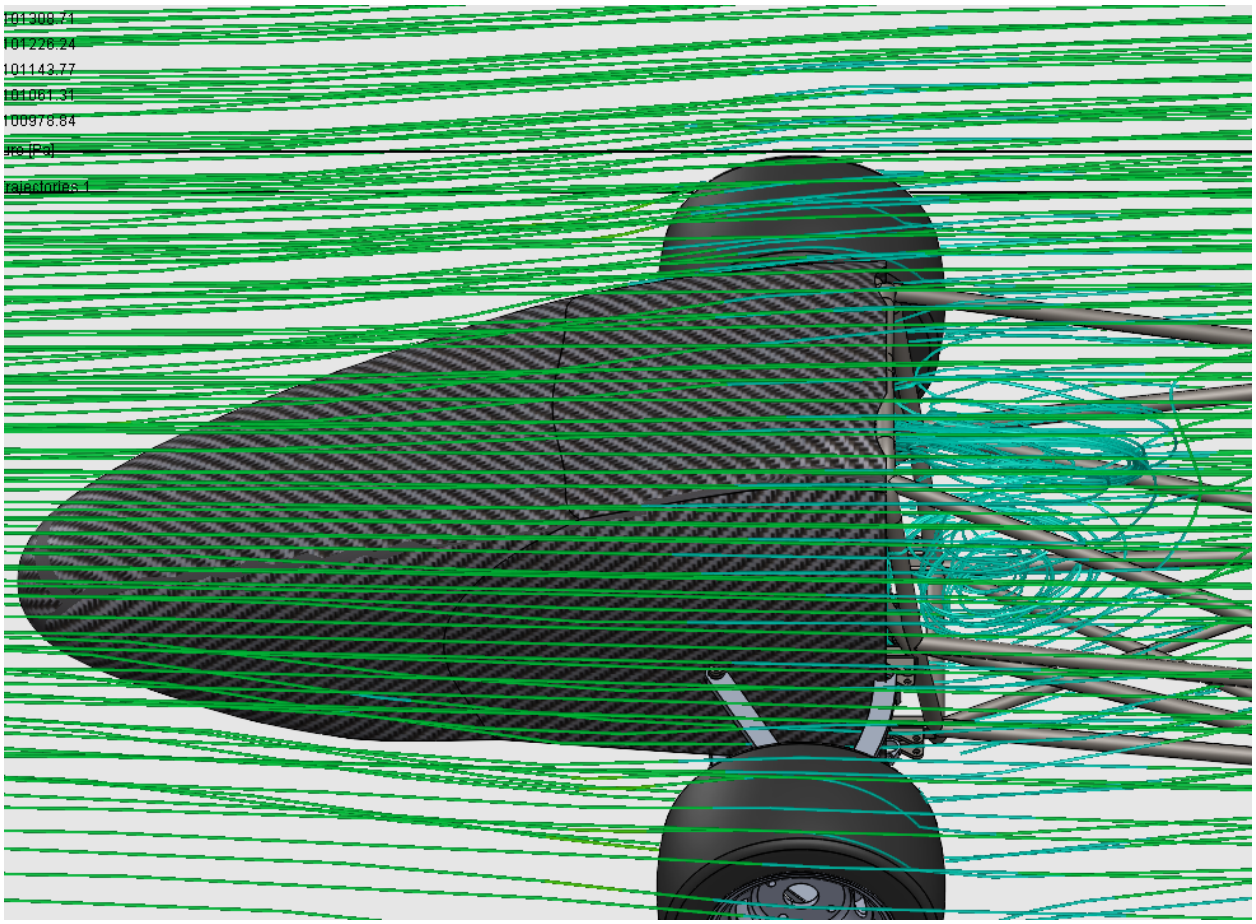

Figure 30: showing the nose cone vortices

The addition of side panels prevented the formation of vortices directly behind the nose cone.

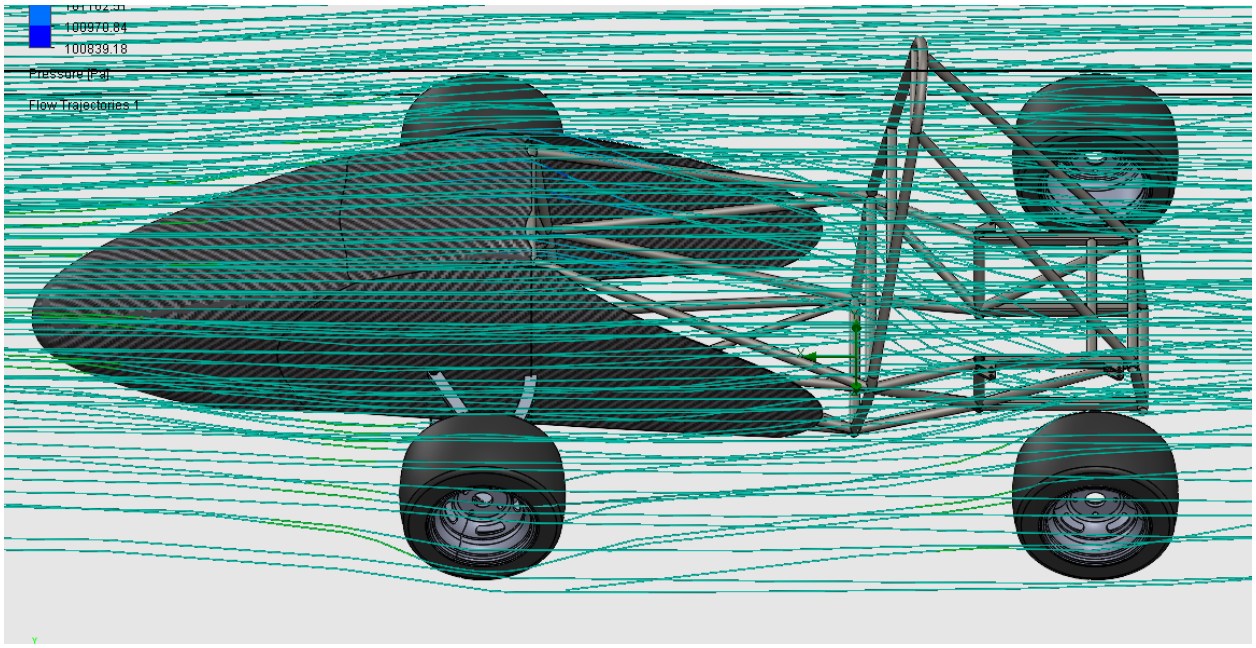

Figure 31: showing side panels eliminate nose cone vortices

The team also evaluated the possibility of adding a rear wing to create downforce, with the goal of improving the car's handling. However, we found that the improvement in handling a wing could provide was not worth the extra weight and complexity. This makes sense, as the car's track speed would not be great enough to generate sufficient aerodynamic downforce. In addition, due to the layout of the car's frame, a rear wing would need to be mounted high up, significantly raising the car's center of mass and increasing its tendency to roll over. Our decision to not include a rear wing is consistent with the team's previous entries, which do not usually build a rear wing for the reasons mentioned.

The team also evaluated the possibility of adding a windscreen, such as in the picture below. The aim would be to shield the driver from debris, and to push the air over the driver compartment, reducing aerodynamic drag. However, we did not succeed in designing a successful windshield; all prospective designs were either impractically large, or created vortices similar to the nose cone, as described above.

Figure 32: A windshield on an FSAE car (Karlsruhe Institute of Technology)

2.5 Exhaust System

For the exhaust system, the team wanted to improve on some of the designs from the 2020 team. This was achieved by redoing some of the calculations and using ANSYS analysis.

P = (850(ED) / RPM) - 3
P = (850(254) / 5500) - 3
P = 36.255 in.
P = (850(254) / 9000) - 3

P = Pipe Length (in.)
ED = Angle range in which exhaust valve is open.

P = 20.99 in.
P = between 21 and 36.25 inches

ID = (√(cc / (P+3)25))*2.1
ID = (√(449.3 / (36.255+3)25))*2.1
ID =1.421 in.
ID = (√(449.3 / (20.99+3)25))*2.1
ID = 1.82 in.
ID = between 1.4 and 1.8 inches

ID = Inner Exhaust Pipe Diameter
cc = Cylinder Volume (cm,3)

The calculations were made in ranges to find the max and min of each value.

In the research conducted on designing an exhaust and muffler system, the ANSYS program was used along with a learning tool to test the designs of the new system.

In order to conduct analysis on a muffler, the desired frequency had to be calculated.

$$\omega = angular\ frequency = units\ of \frac{radians}{sec}$$

$$\omega = rpm * \frac{2\pi \frac{rad}{rev}}{60 \frac{sec}{min}}$$

This formula was used to calculate the frequency required in radians per second and was then converted to hertz. When the analysis tool started up, the frequency was way too high to be in the band of values needed for this engine (Figure 33). The geometry was changed to accommodate for this. In this tool, there were 4 bodies that made up the muffler: the outer shell made of sheet steel (materials calculations were conducted on all parts of the design), an inner foam with holes, an inner metal tubing with holes, and the cylinder of air in the center. The holes were adjusted for the desired frequency.

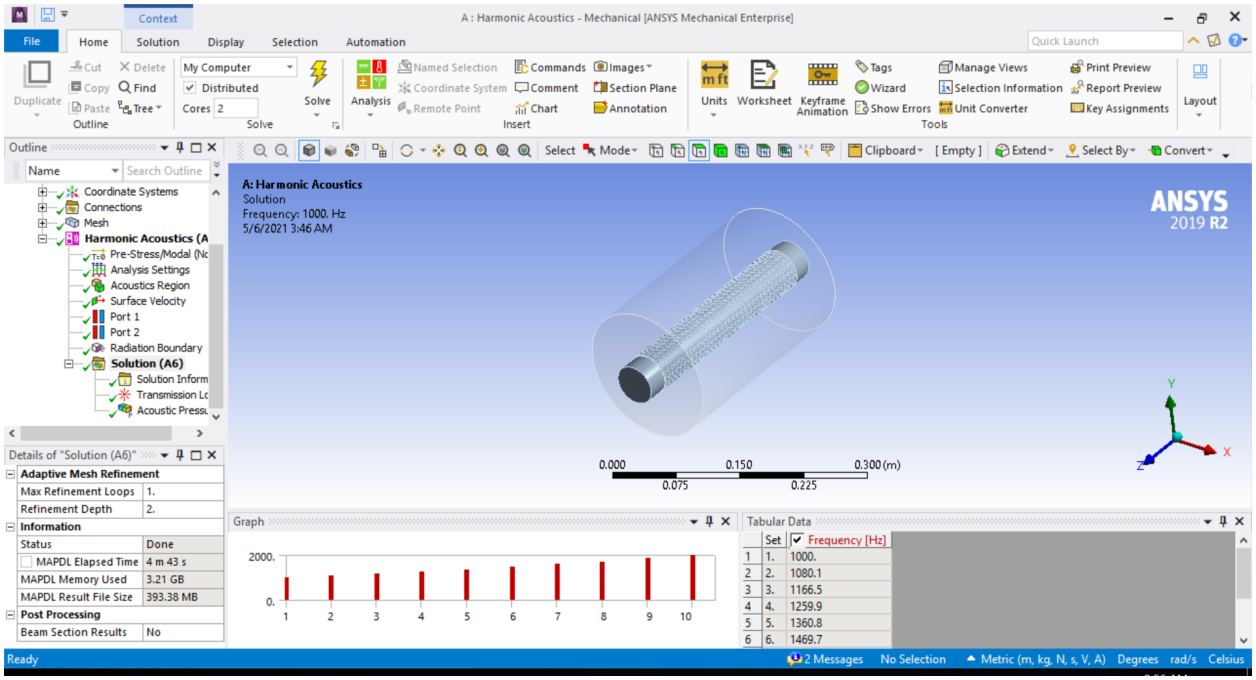

Figure 33: Startup of Analysis Tool

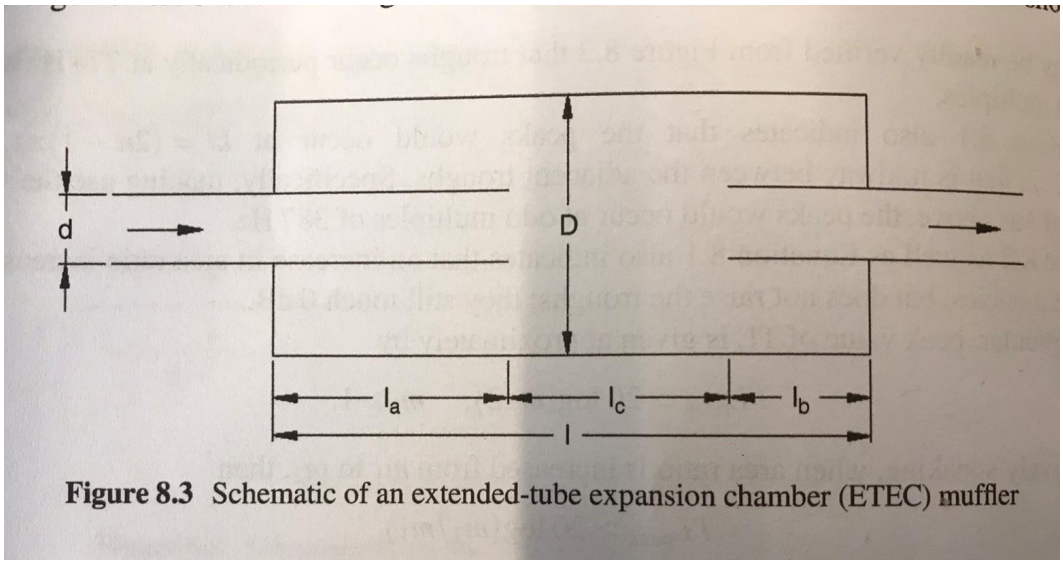

Figure 8.3 Schematic of an extended-tube expansion chamber (ETEC) muffler

Figure 34: Schematic used to Model the Muffler (Ansys Learning Forum)

2.6 Lap Simulation

If our car was to compete at competition, three of the dynamic events our car will compete in are an acceleration, autocross, and endurance event. The goal was to provide the team with a simulator that could model each of these events. The University of Wisconsin Madison provided documentation on the vehicle dynamics to create such a simulator. Wanting to start with the fundamentals and work up to an advanced simulator, a point mass was modeled and graduated into a bicycle model.

Once a working bicycle model was developed, it was clear it would be very intensive to further develop this model into a two-track auto-cross simulator. As a result, another method to create an auto-cross simulator at a point mass level was considered. Ultimately a paper by James Hakewill was used as the base for creating the point-mass autocross simulator.

Although the initial scope was to make this one tool, the club now has two that are used for different purposes. One models the acceleration event as a bicycle-model, and the other models autocross and endurance events as a point mass. The Acceleration Simulator was built to be based on a set change in time (dT), while the Autocross Simulator was built on distance covered. This discrepancy works in favor of each event, as the acceleration is evaluated on time with a set distance and the autocross and endurance events are over varying distances.

Point Mass Acceleration Simulator

As previously mentioned, this simulator started out as a point mass. The goal of starting the model with a point mass was to create a controlled body that is traction limited, and accelerates in one direction. From here, aerodynamic effects could be added, such as downforce and drag forces, which would alter the previously linear acceleration of our car. Acceleration was no longer just a function of the coefficient of friction and gravity. It now accounted for the

changes in downforce and the force of drag prohibiting the body from accelerating.

At this point, our body was accelerating at the traction limit. The next step was to compare the capability of the motor to this traction limit, and use the smaller force to accelerate the body. This essentially added traction control to our model, and prevented simulation of spinning the tires as the motor capability would be greater than the friction limit.

Bicycle Model Acceleration Simulator

To increase the validity of the simulator, the point mass was then given longitudinal weight transfer capability to make it into a bicycle model. With two points in contact with the ground, a moment is created around the center of gravity under acceleration. Thus, the calculated weight transfer indicates how much normal force needs to be removed from the front tire and applied on the rear (vice versa under braking). Introducing this into the simulator created separate calculations for the front and rear axles, thus we could now evaluate the effect of having individual hub motors on future FSAE cars.

General Calculations				*Aero and Wtransfer*		
time	Distance	velocity	Acceleration	Fdownforce	Fdrag	Wtlong
0	0	0	0	0	0	0
0.1	0.01	0.1	#DIV/0!	0	0	0
0.2	0.157341	1.473406	13.7340587	0.0208725	0.0104363	0
0.3	0.442149	2.84808	13.7467442	4.5312629	2.2656315	686.70294

Front Wheel Calculations				Rear Wheel Calculations			
Fn,Front	Ffriction,Front	Fmotor,F	Fcp,F	Fn,Rear	Ffriction,Rear	Fmotor,R	Fcp,R
1412.64	1977.696	0	0	1726.56	2417.184	0	0
1412.64	1977.696	#DIV/0!	#DIV/0!	1726.56	2417.184	#DIV/0!	#DIV/0!
1412.649	1977.70915	11368.18	1977.709	1726.571	2417.200072	10813.64	2417.2
727.9761	1019.166586	11368.18	1019.167	2415.755	3382.057182	10813.64	3382.057

Figure 35: Output data channels from the lapsim

The Acceleration Simulator output channels are shown in Figure 35. While the time channel is our reference for evaluating performance in this event, we can evaluate how car parameters affect channels outlining our induced forces, velocity, and acceleration values.

Autocross Simulator

With time restraints, the autocross simulator was kept as a point mass. The vehicle dynamic equations used were very similar to those used in the acceleration sim, with more constraints. To make our point mass act as a real accelerating body, the following limitations were imposed:

- Limiting friction equation for maximum speed around a given radius curve
- Limiting engine from exceeding maximum frictional force (traction control)
- Apply a braking force in previous sectors, entering a corner at max speed
- Limiting engine speed from rising past its max capability

As the body accelerates from a slow speed, the sim doesn't let any tire spin occur. Then as it is accelerating, it uses the drag force to restrict max speed approaching a corner. At a corner, the sim resets its entry velocity to the max velocity which can be sustained with that corner's radius. Finally, the velocities are revisited to apply braking force leading up to the corner entry.

Being our first year creating our own lap simulation tools, we have no x-y coordinates of an FSAE track logged. As a result, no simulation runs could be completed that we knew would be completely accurate. Using Matlab and the FSAE course description in the rules, a program was created to plot a theoretical FSAE track (Figure 36).

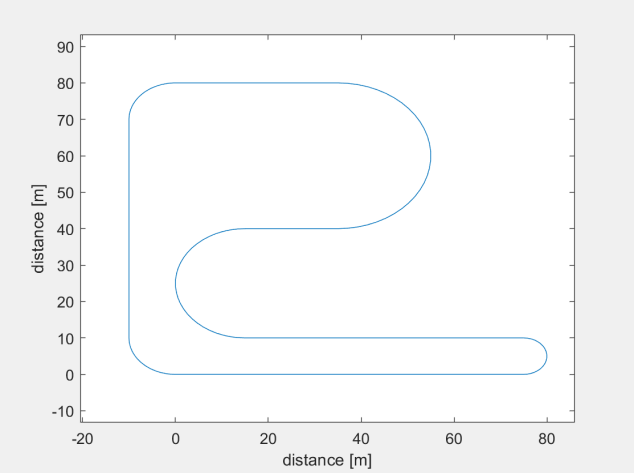

Figure 36: Track used in Autocross Simulator created in Matlab

This track included a corner of the minimum and maximum radius, and the longest maximum length straight away. Currently the data logging system is set up to record gps locations. After a competition, we will be able to update our SIM with an actual FSAE track layout and increase our accuracy.

Section 3: Manufacture and Assembly

3.1 Suspension

At this point, all of the components that need to be machined are done or in progress. Depending on the part, the process for machining was very similar. First, the part model is inspected for machinability and the necessary changes were made. Then, the model was imported into ESPRIT and files were created with all operations. The fixturing was then designed and the parts were machined on a CNC. Most of the parts were then finished by hand.

The rear uprights were already machined by last year's team. All that had to be done were the drilling and tapping of the holes. To accomplish this, 4 different operations were used. Figure 37 shows the orientations of the uprights in the VM2. In order to fixture it to the machine, an L-Plate, 1-2-3 Block, mounting brackets and a dial indicator were used (Figure 38).

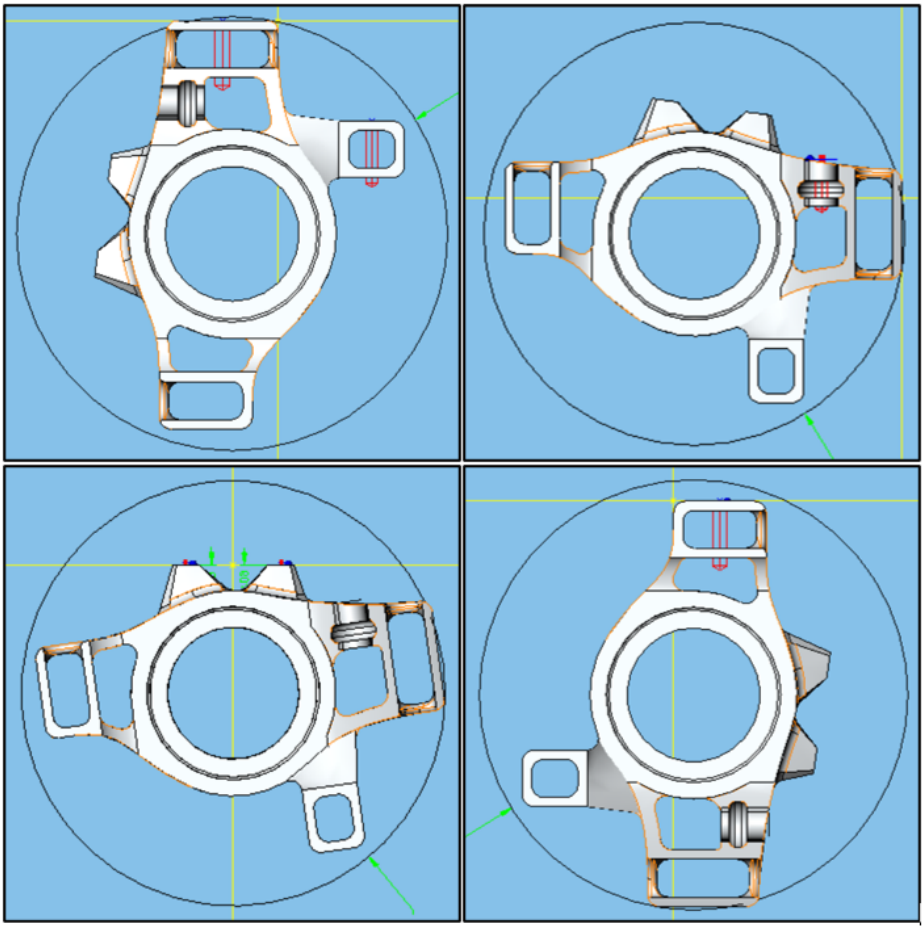

Figure 37: All Orientations Used to Drill the Holes

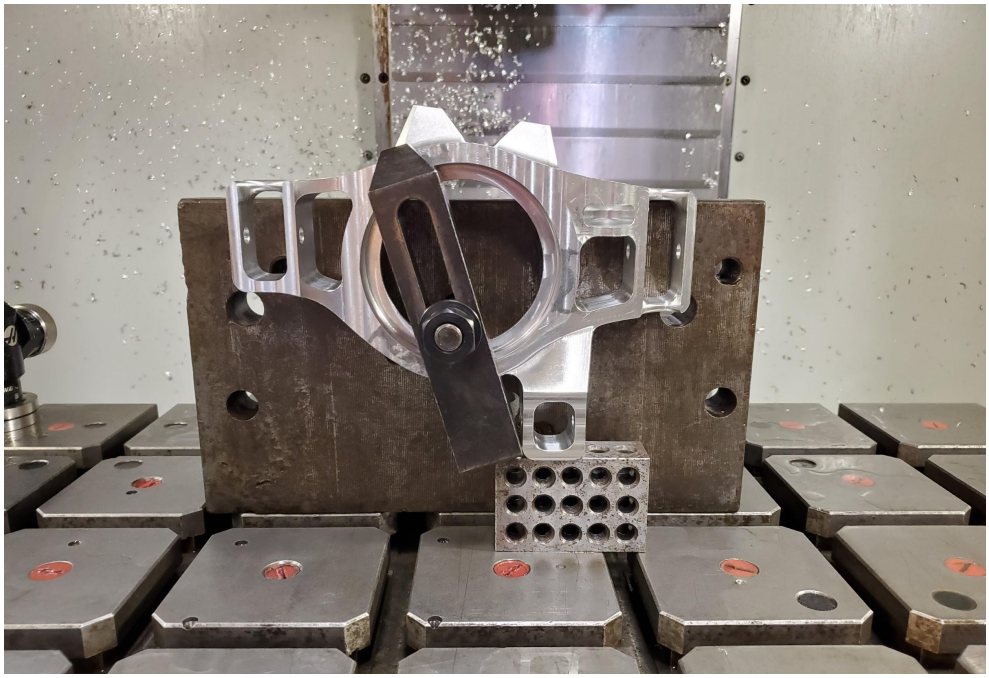

Figure 38: Mounting of the Rear Uprights

Figure 39 shows a different form of fixturing this part. The hole that needed to be drilled did not have a parallel surface on the top face to ensure it is level in the fixture. The purple line shows where the hole needed to be drilled. In order to fixture and probe this part, a different parallel face would have to be used. Unfortunately the only face was directly under it (blue line Figure 39). to fixture this part, a dial indicator was used on this face to ensure it was level. To probe, however, a ruler was measured using calipers, placed in this pocket, and then the rulers' face was probed. Then, the difference was subtracted from that, and that surface was used as zero.

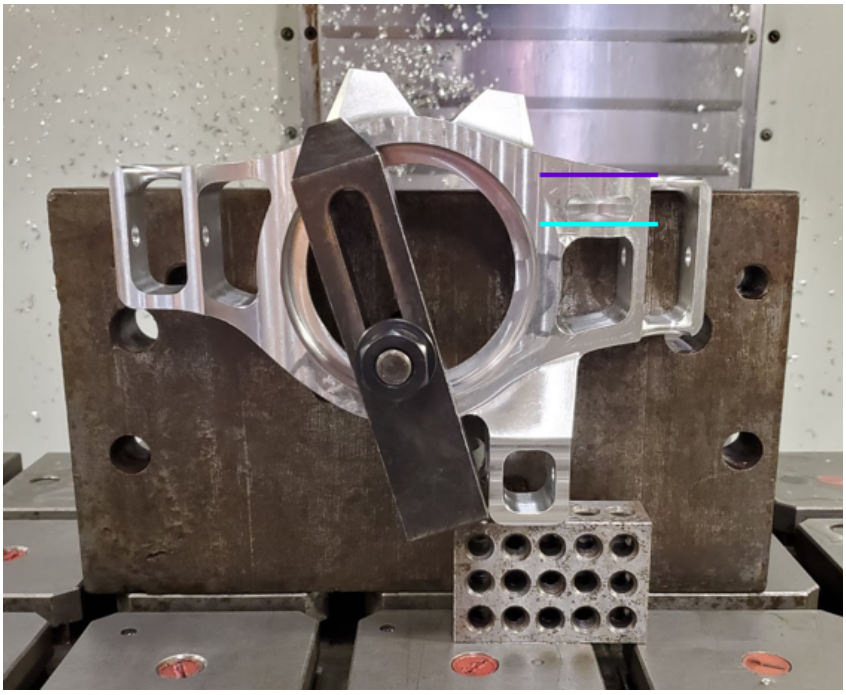

Figure 39: Rear Upright with Indicator Lines

In the redesigning of the control arms, it was determined that a tube cross section would be best. As stated in the design section, the blanks were cut out of 0.5in diameter 4130 steel tubing. Since they are steel, a horizontal band saw (Figure 40) was used to cut the control arms to their specified length plus an additional 1/8th inch. This was to accommodate for the width of the blade and to have enough space to put a bevel on one end using a lathe (Figure 41). The bevel is to ensure ease of welding.

Figure 40: Control Arm Rods Being cut in the Horizontal Band Saw

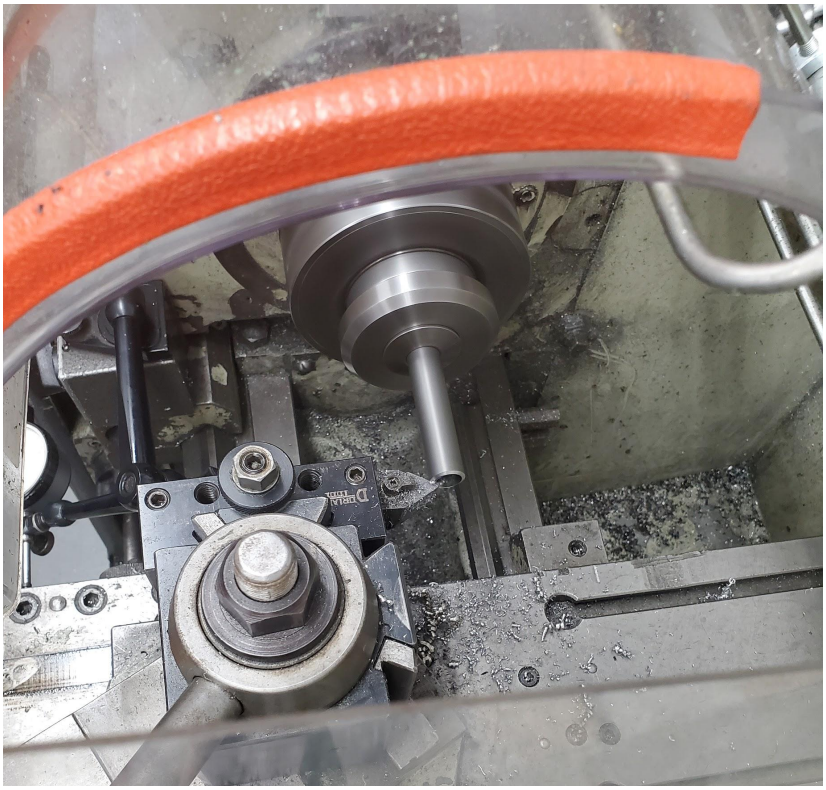

Figure 41: Control Arm Rod in Lathe getting a Bevel

For the front rockers, some of the features had to be changed for machinability (Figure 42). Both the front and rear rockers were machined using the VM2.

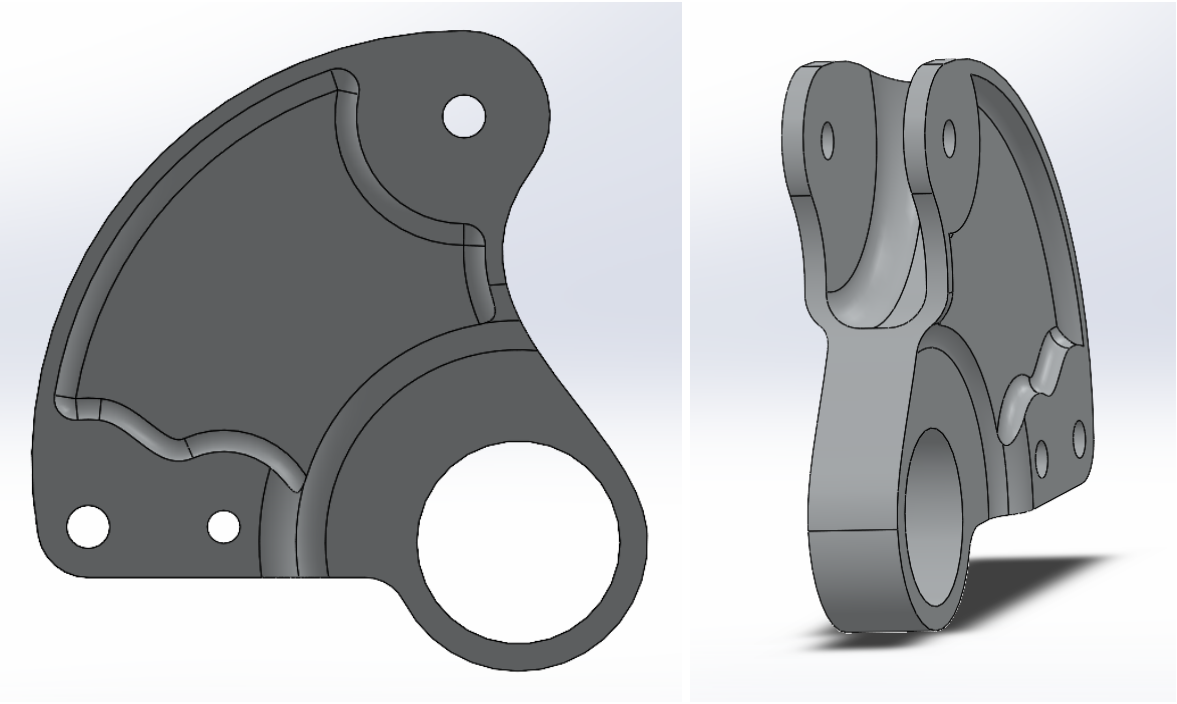

Figure 42: Front Rockers with Improvements

3.2 Engine and Drivetrain Mounting

All of the steps within the mounting process of the engine and drivetrain is complete or nearing completion. The engine itself is securely mounted at six points, two in the rear, two on the top, and two on the bottom. Each of these points are connected to the larger mounts by way of ⅜" thick threaded rod, with ⅜" thick rubber bushings, washers and lock nuts. The full assembly is shown below:

Figure 43: Rear Engine Mount Connection

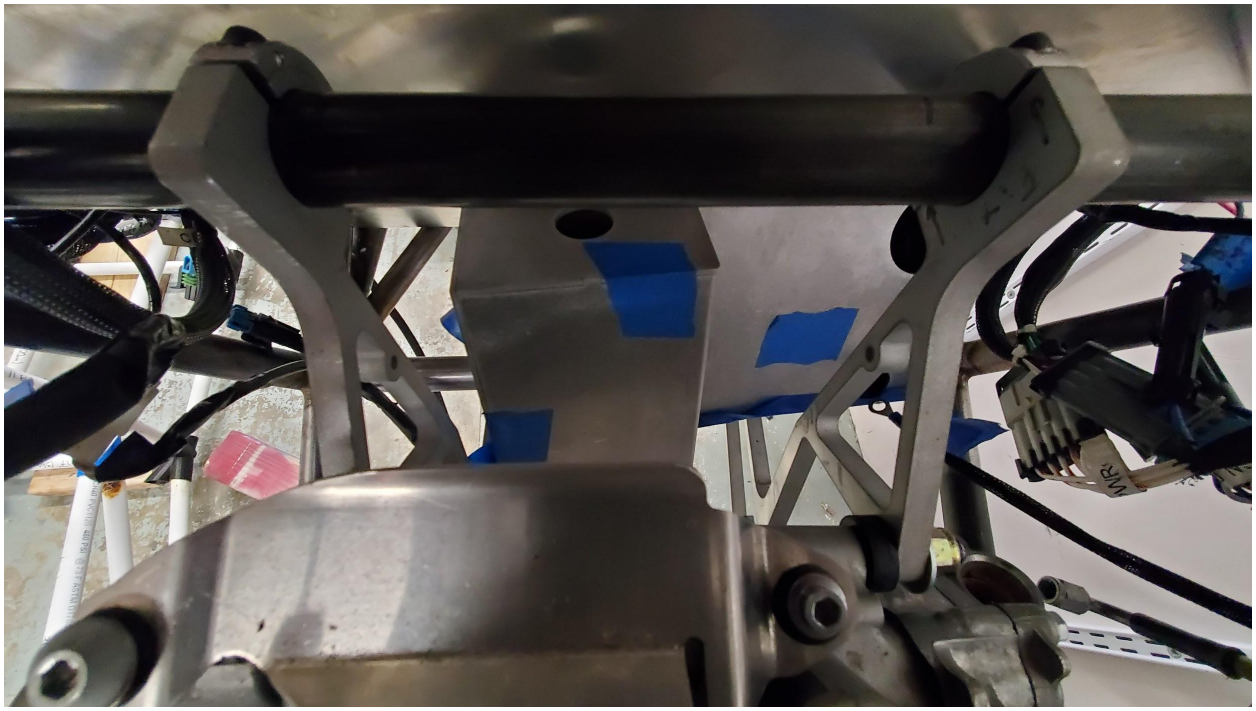

Figure 44: Top Engine Mount Connection

The engine was mounted such that the center of mass for the engine is in line with the center of the frame, in order to prevent any issues with weight distribution inequalities. The Drexler non-adjustable differential will mount behind the engine, and when positioned correctly, the drive chain will be perpendicular to the frame itself. The differential mounts are waterjet from a 10mm thick 7075 plate, using the facilities at Hydrocutter in Oxford, MA. The mounts themselves slide over machined collars, and are tightened by way of 8mm bolt and nut.

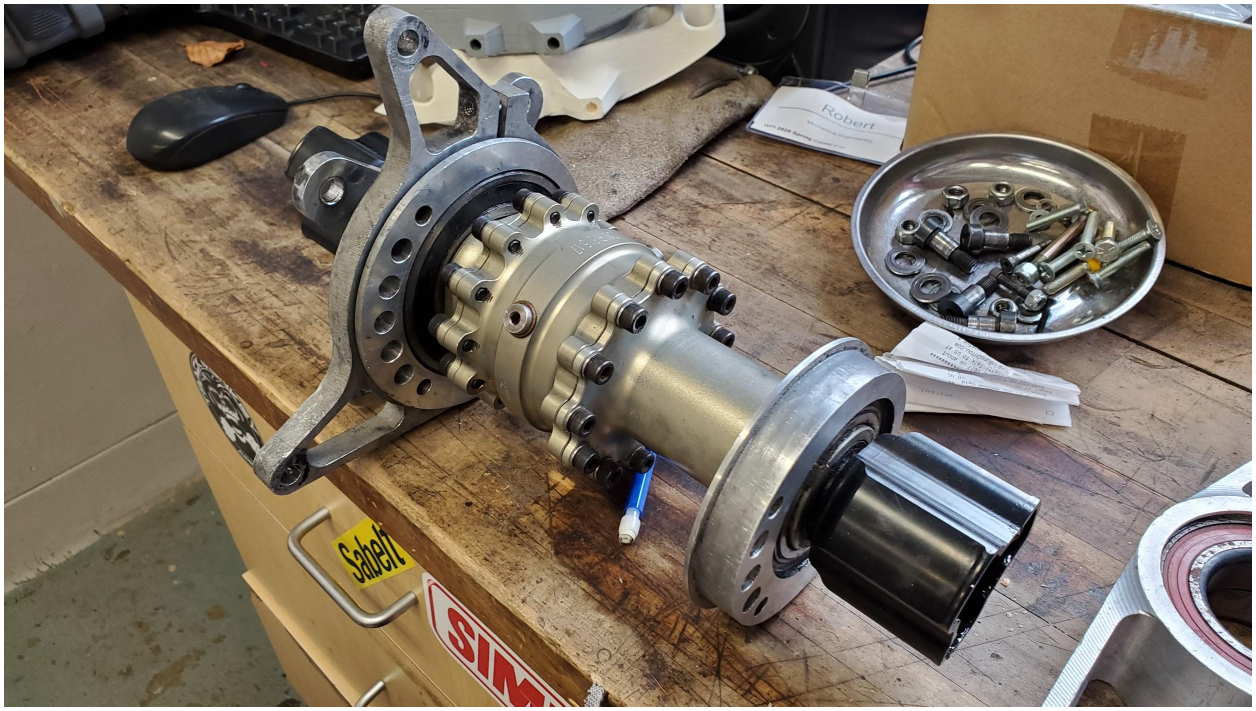

Figure 45: Drexler Differential With Mounting Collars

3.3 Braking

For the brake rotors, they started off in 9.5”dia by a variable thickness of 0.27” - 0.4” (Figure 46). Due to the variable thickness, it was decided that a manual drill mill would be used to first flatten the blanks to about the same thickness using a face mill (Figure 47). The front ones were milled down to a thickness of 0.29” and the rear ones to 0.19”. The two different

thicknesses were because the front and rear calipers have different spacing between the brake pads. Then, the VM2 was used to cut the internal pattern into the blanks (Figure 48). The mounting for this is also shown in Figure 48 using clamps and a sacrificial bottom piece. To get the outer diameter, they were put on the manual lathe and cut down to size (Figure 49). Originally, when all of the features were complete, they were going to be finished on the surface grinder in pairs to ensure they're even, however, the bed to the grinder was too small, and the finishing operations will have to be done on a CNC using a more precise face mill on both sides to prevent warping.

Figure 46: Rotor Blanks

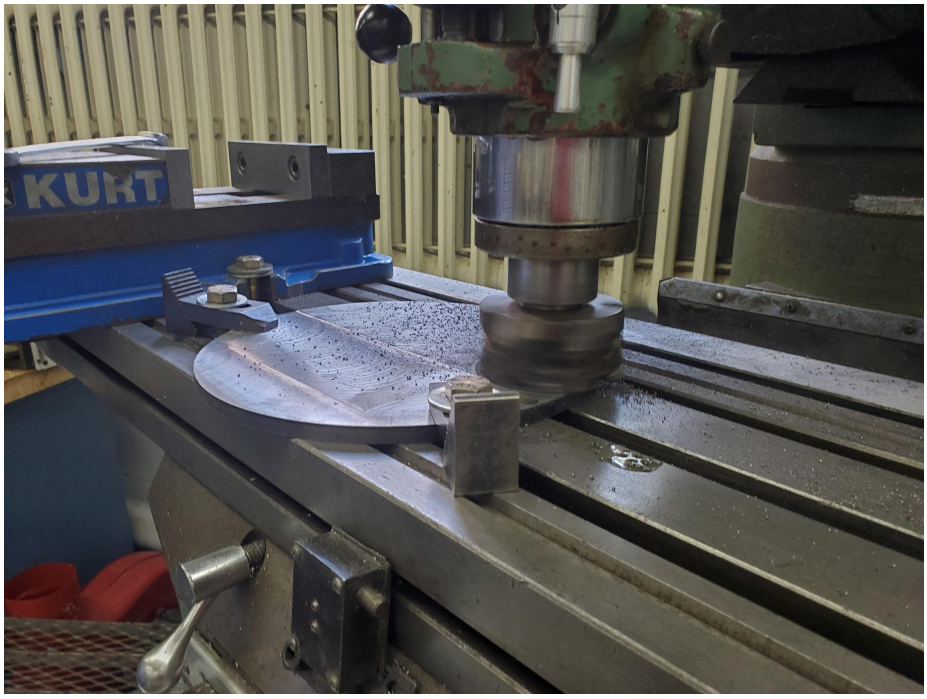

Figure 47: Brake Rotor Blank in the Manual Mill

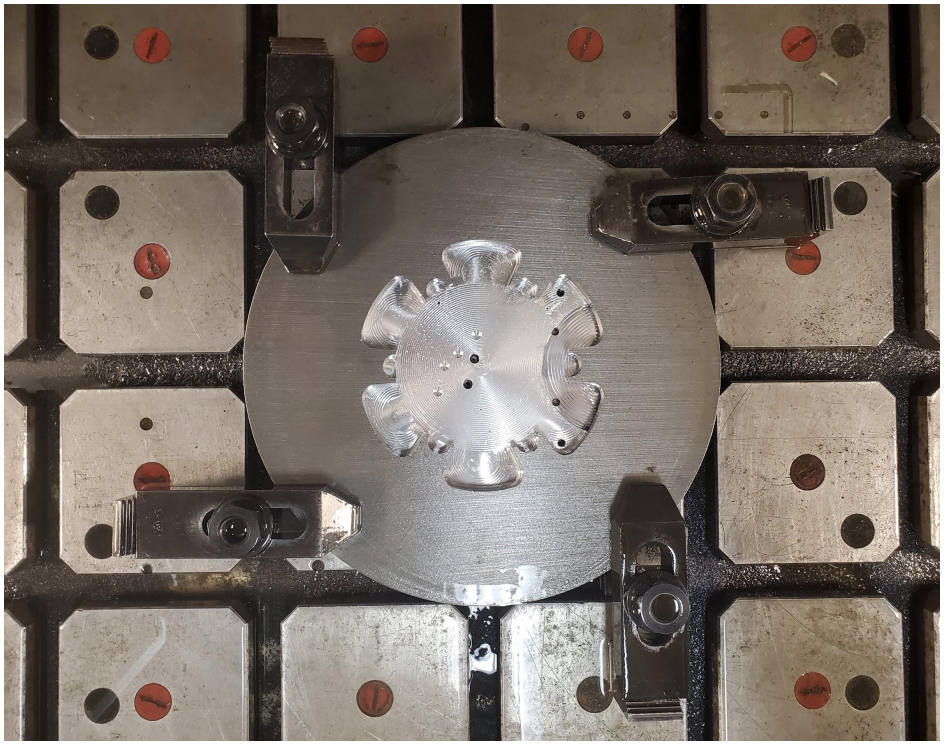

Figure 48: Brake Rotor in the VM2

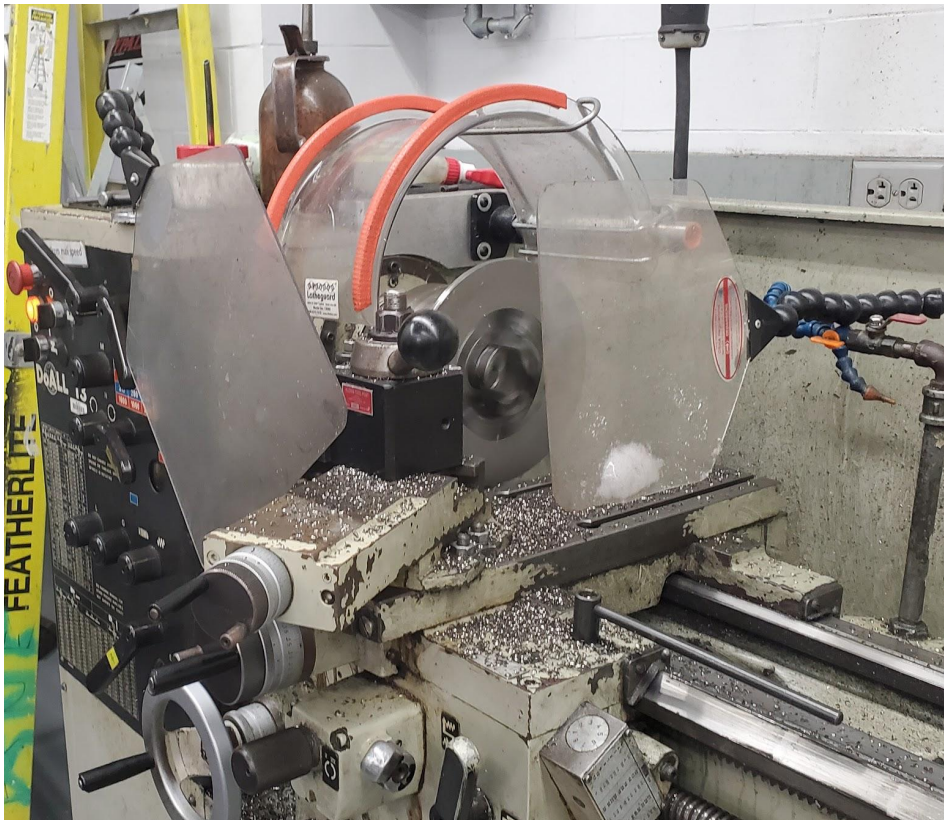

Figure 49: Brake Rotor on the Lathe

Section 4: Conclusions and Future Works

4.1 Limitations

The largest limiting factor in the team's ability to make progress in this project was the restrictions put in place on WPI's campus due to COVID-19, especially early in the year. Because it took several months for the team to get access to the FSAE lab, it was difficult at first to even examine the car and assess its current state. In addition, this year's team was significantly smaller than that of previous years. As a result, the window of time in which the team could meaningfully progress was shorter than in a typical school year, and we were able to make less progress.

This car was originally meant to be completed by last year's MQP team, and so they did not document their work with the intention that another group would need to familiarize themselves with the details of their project and then complete it. That, combined with the rushed departure from campus in spring 2020, meant that a significant amount of this year's team's time was spent familiarizing ourselves with the work of last year's team.

4.2 Future Work

4.2.1 Suspension

*FSAE Club members, please reference the 2019-2020 final report for additional information on manufacturing techniques, and their design decisions

<u>Control Arms-</u>

- Weld the A-arms into the gussets
- Weld the inserts into the control arm ends
- Purchase and install end links from McMaster-Carr with model number 60645K14

- Attach to control arm tabs on the frame per appropriate mounting hardware

Pushrod Rocker System-

- Weld a nut on each end of every pushrod
- Thread in the appropriate end links stocked in the FSAE shop
- Visit the 2020 damper calculations to make an appropriate spring choice

Uprights-

- Finish the machining process of the front uprights

4.2.2 Engine and Drivetrain Mounting

For the next FSAE MQP Team, engine mounting is completely finished. There may need to be final adjustments to properly align the engine and differential once both are fully mounted, but this is unlikely and relatively easy. The differential mounting brackets are waterjet but still need to be machined. The old steel tabs from the previous MQP team need to be ground off to make room for the new mounts. After the frame has been returned to its original state, the differential mounts are assembled in much the same way as the engine mounts.

4.2.3 Braking

All of the system has been fully designed and the rotors have been manufactured. The brake pedal, brake pedal bracket, and the master cylinder brackets need to be machined.

4.2.4 Aerodynamics

For the next FSAE Team, all aerodynamic surfaces need to be manufactured. In addition, much of the reason that a rear aerodynamic package was not designed was out of consideration for the time it would take to make; if future teams have more time, it may be worth it for them to re-evaluate the feasibility of designing and manufacturing a rear wing and / or an engine cover.

Future teams may also have success in designing a windshield; just because we were not successful in creating a design that was able to shield the driver and provide aerodynamic benefit does not mean that it is impossible to do so.

4.2.5 Exhaust System

Most of the material needed to make the exhaust system is in the shop. The next team will have to manufacture the piping and the muffler.

Section 5: References

Duff, R., Williams, J., Ingegneri, A., Meaasmer, J., Pedro de Vasconcellos, Pellerin, M., & Sanborn, E. (2020). (rep.). *Design and Optimization of an FSAE Vehicle*.

Engine mounts: The complete guide. Muir, A. (Director). (2019).[Video/DVD] howacarworks.com.

Formula SAE. (2021, January 1). https://www.fsaeonline.com/cdsweb/gen/DocumentResources.aspx.

Gillies, M. (2020, November 13). *Chaparral 2E*. Car and Driver. https://www.caranddriver.com/features/a15388275/chaparral-2e/.

Karthik, S., Krupa, R., & Smruti Rekha, S. (2016). Design and Analysis of a Pushrod Suspension System for a Formula Racing Car, *2*(2).

Ketsatis, G. (2021, April 7). *The 1921 Rumpler Tropfenwagen*. Collectorscarworld. https://collectorscarworld.com/how-the-1921-rumpler-tropfenwagen-foreshadowed-todays-mid-engine-race-cars/.

Lord, H. C. (1930). ‘Vibration dampening mounting

Milliken, W. F., & Milliken, D. L. (1995). *Race car vehicle dynamics*. Society of Automotive Engineers.

Marjoram, R. H. (1985). Pressurized hydraulic mounts for improved isolation of vehicle cabs. SAE Paper #852349,

SAE. (2020). FSAE student events. Retrieved from https://www.sae.org/attend/student-events

Tiwari, A., More, S., & Shahane, A. (2018). STUDY OF ROAD HOLDING AND RIDE COMFORT ANALYSIS WITH THE HELP OF QUARTER CAR MODEL, *3*(12).

Vadhe, A. A. (2018). Design and Optimization of Formula SAE Suspension System. *International Journal of Current Engineering and Technology*, *8*(3).

Vijayenthiran, V. (2012, August 12). *Audi Recovers Missing 1939 Auto Union Type D*. Motor Authority. https://www.motorauthority.com/news/1078397_audi-recovers-missing-1939-auto-union-type-d.

Yu, Y., Peelamedu, S. M., Naganathan, N. G., & Dukkipati, R. V. (2001). Automotive vehicle engine mounting systems: A survey. Journal of Dynamic Systems, Measurement, and Control, 123(2), 186-194. Retrieved from https://doi.org/10.1115/1.1369361